Testing the Antlia Quadband Anti-Light Pollution Filter

by Jim Thompson, P.Eng
Test Report – November 18th, 2023

Introduction:
The search for the best all-purpose filter continues, with new developments coming on a seemingly monthly basis. Creating a filter that can improve the contrast of all object types, both nebulae and galaxies, is a challenge that several filter manufacturers (OEMs) have decided to take on. In May of this year, I released a test report comparing the new Antlia Triband RGB Ultra and IDAS GNB to other pre-existing filters. The marketing material for both filters touted them as improving the view of all types of objects. The outcome of my testing was to confirm the IDAS GNB as the best performing all-purpose filter. However, in that same test report I introduced a filter concept that had the potential to perform better than the GNB. To the benefit of amateur astronomers, Antlia has made that filter concept a reality and have released it under the name Quadband Anti-Light Pollution or Quad-ALP for short. Evaluation of this new filter is the focus of this test report.

Objective:
The objective of this test report is to evaluate the performance of the new Antlia Quad-ALP, comparing it to other existing filters of the same type. The list of filters considered in this test report is provided below and is illustrated in Figure 1 (quoted price for 2" version):

- Astronomik UHC – $170USD
- IDAS DTD – $198USD (by analysis only)
- IDAS NB-1 – $150USD
- IDAS GNB – $258USD
- Antlia Triband RGB Ultra – $179USD
- Antlia Quadband Anti-Light Pollution – $198USD

The UHC filter has been included since it has for many years held the title of best all-purpose filter amongst the electronically assisted astronomy (EAA) community. I don't have a sample of the DTD to test but I have a copy of the OEM's spectrum for the filter, so I am able to include it in my performance predictions. All the filter samples to be tested were purchased by me from various vendors. Note that at the time I purchased the IDAS GNB filter, it was only available in "ZF" format. Filter performance was evaluated based on the increase in contrast between the observed object and the background, which is a measurable quantity. It was evaluated quantitatively using the measured filter spectra combined with the spectra of several common deepsky objects, and by direct measurement from images captured using each filter and either a one-shot colour (OSC) or a monochrome camera. The spectrometer and image data was also used to evaluate the signal-to-noise ratio (SNR) achieved using each filter.

Figure 1 Photos of Filters Under Test

Method:
Testing consisted of data collection from the following sources:

- Spectral transmissivity data, from near-UV to near-IR, measured using an Ocean Optics USB4000 spectrometer; and

- Image data, collected using the following setups:
    - Askar FMA230 apochromatic refractor (f/4.6) with ZWO ASI533MC Pro camera;
    - William Optics ZS66 ED doublet refractor (f/5.9) with ZWO ASI533MC Pro camera.

The spectrometer data was collected in my basement workshop with the USB4000 and a broad-spectrum light source. Filter spectra were measured for a range of filter angles relative to the light path, from 0° (perpendicular) to 20° off-axis. The spectrometer was recently upgraded, replacing the entrance slit and diffraction grating, to give a wavelength resolution of 0.5nm.

For the purposes of predicting the relative performance of each filter using their measured spectra, a reference spectrum was established for the typical observing objects: bright O-III rich emission nebulae, faint H-α rich emission nebulae, galaxies, reflection nebulae, and comets. The normalized emission spectra used in the analysis are plotted in Figure 2. Reference data used to produce these spectra was found in publicly available resources online, the source object in each case being as follows:

- O-III rich nebulae: M27
- H-α rich nebulae: NGC7000/M42/M8
- galaxies: M51
- reflection nebulae: M45
- comet: combination of 8 different comets from various sources

The image data was collected from my backyard in central Ottawa, Canada where the naked eye limiting magnitude (NELM) due to light pollution is +2.9 on average (Bortle 9+). I switched filter configurations using a ZWO 2" filter drawer. Each time I changed filters I refocused on a conveniently located bright star using a Bahtinov mask. Images were collected on three different evenings as described below.

1. October 30th, 2023: FMA230+ASI533, target M31 "Andromeda Galaxy";
2. November 10th, 2023: FMA230+ASI533, targets IC405 "Flaming Star Nebula", M45 "Pleiades", & NGC2244 "Rosette Nebula";
3. November 12th, 2023: ZS66+ASI533, targets M31 "Andromeda Galaxy", M33 "Triangulum Galaxy", IC434/NGC2024 "Horsehead & Flame Nebulae", M42/NGC1977 "Orion & Running Man Nebulae".

A Moon two days past full was in the sky during my October 30th imaging session, but the other two sessions took place around the new Moon.

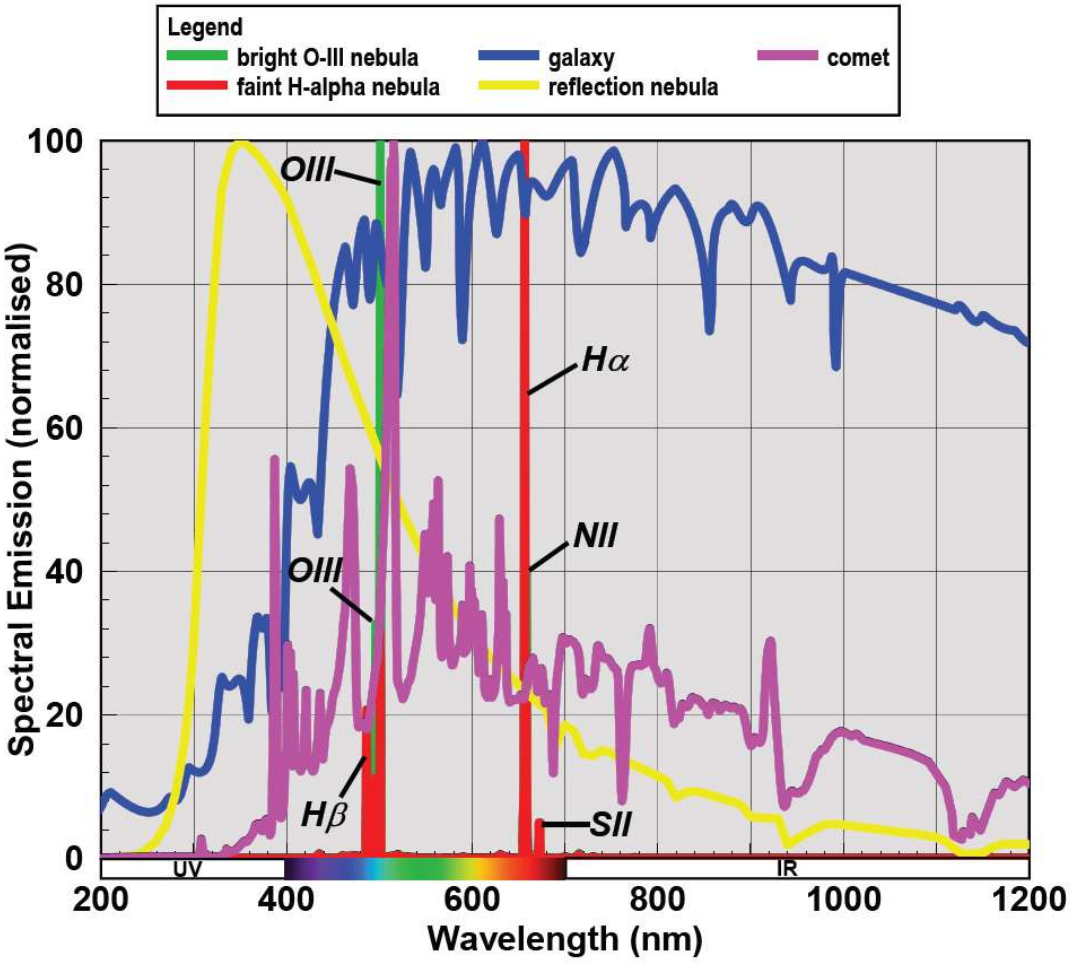

Figure 2 **Normalized Emission Spectra for Typical Observing Targets**

Results –Spectrum Measurements:

Using the test method mentioned above the spectral transmissivity for each filter was measured for a range of filter angles relative to the light path. Figures 3 to 5 present a plot of each filter's resulting spectral transmissivity data for the case of the filter perpendicular to the light path. All the filters tested were shown to have high transmission values (>90%) at the important wavelengths for nebula emissions. Several of the filters also have a pass band at the blue end of the spectrum, but of varying bandwidth depending on the particular filter. Some of the filters also pass infrared light, again to a varying extent depending on the filter.

All the filters tested have wide pass bands as can be seen in Figures 3 to 5. As a result, they all have very low sensitivity to the angle of the light passing through the filter. One can expect consistent performance from any of the filters tested down to f-ratios at least as fast as f/2.

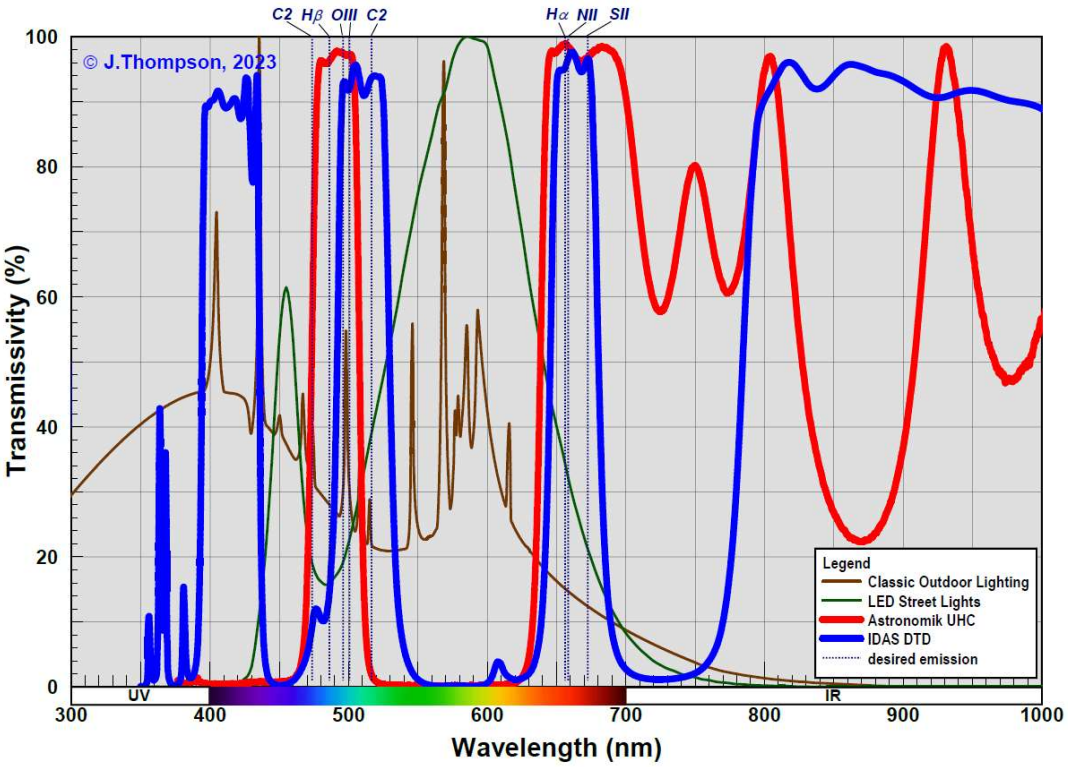

** IDAS DTD spectrum from OEM*

Figure 3 Measured Spectral Response of Tested Filters – UHC & DTD*

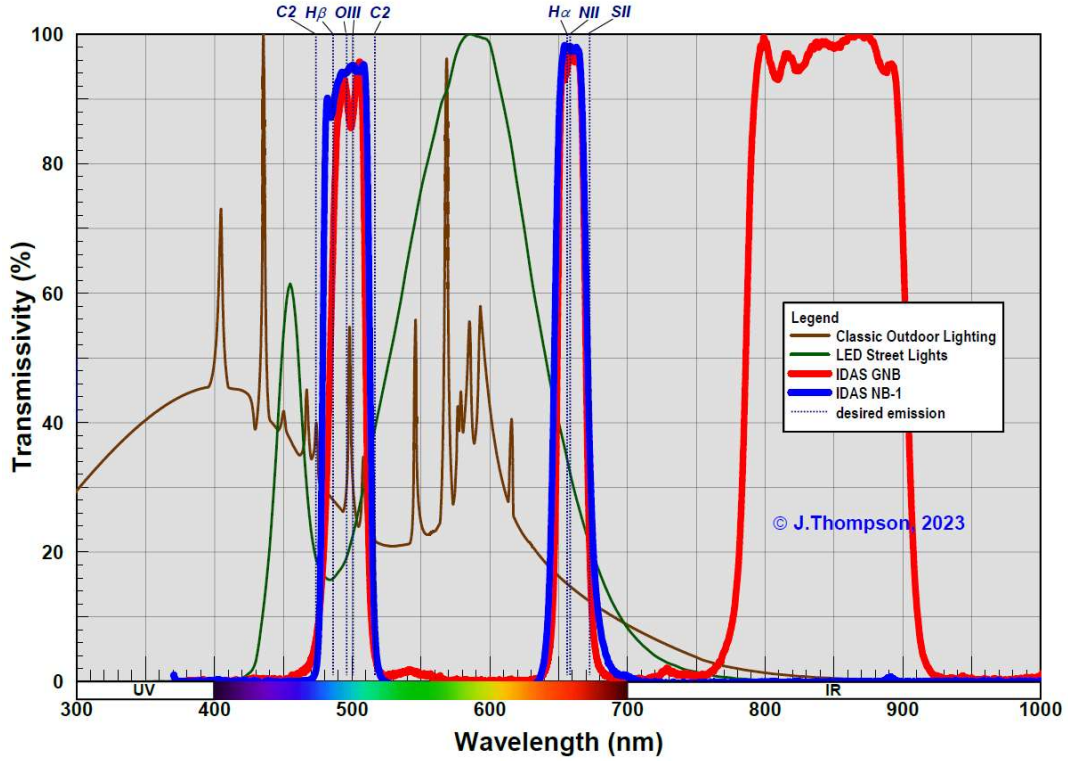

Figure 4 Measured Spectral Response of Tested Filters – GNB & NB-1

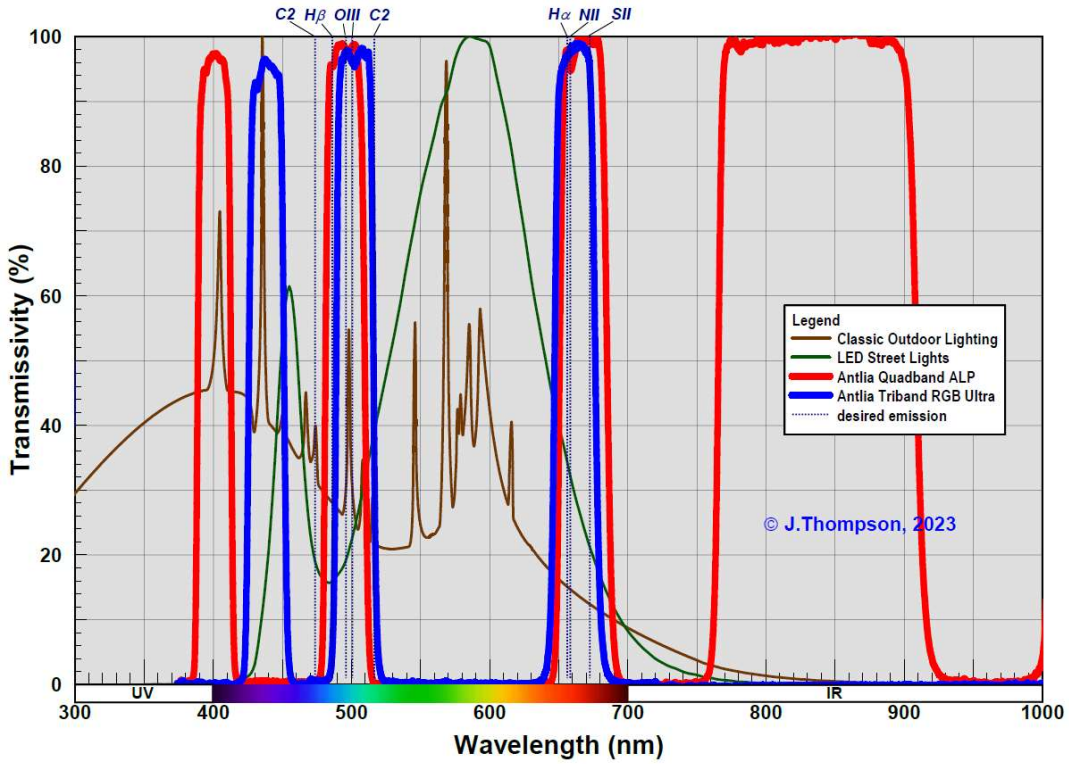

Figure 5 Measured Spectral Response of Tested Filters – Quad ALP & RGB Ultra

With the filter spectra in hand, it was possible to extract overall performance related statistics for each filter, such as transmission values at key wavelengths of interest. The filter statistics are provided in Table 1, including a calculated value for percent Luminous Transmissivity (%LT), a single number that describes generally how much light is getting through the filter. The calculated value of %LT depends on the spectral response of the detector, which in this case is assumed to be a modern back illuminated CMOS sensor. The six emission wavelengths of interest for emission nebulae are included in Table 1 (H-β, O-IIIa & b, H-α, N-II, S-II), as well as some key wavelengths associated with comets (CH, Swan C2 bands) and an average transmission in the near infrared (700 to 1000nm).

Filter	%LT*	CH (387)	C2 (471.5)	Hbeta (486.1)	O-IIIA (495.9)	O-IIIB (500.7)	C2 (516.5)	C2 (563.5)	Halpha (656.3)	N-II (658.4)	S-II (672.4)	NIR
No Filter	100	100	100	100	100	100	100	100	100	100	100	100
Astronomik UHC	36.0	0	25	96	97	97	2	0	99	98	97	59
IDAS DTD	35.5	2	6	14	92	92	93	0	95	97	96	59
IDAS GNB	19.5	0	3	63	91	88	4	0	95	97	27	39
IDAS NB-1	12.3	0	0	84	92	94	17	0	98	99	49	0
Antlia Triband RGB Ultra	17.5	0	1	5	97	96	38	0	97	98	96	0
Antlia Quadband ALP	28.6	8	0	95	98	98	0	0	97	95	99	48

* calculated assuming spectral QE curve for IMX174M with no UV/IR blocking filter

Table 1 Measured Filter Performance Summary (% Transmission)

Knowing the measured spectral response of the sample filters also allowed me to predict the theoretical relative performance of each filter when imaging different types of object. To do this I used the method I developed back in 2012 which applies the spectral response of the filter and sensor combined with the spectral emission from the object (Figure 1) and background light polluted sky to estimate the apparent luminance observed. To help visualize the results of this analysis I have plotted the predicted % increase in contrast (vs. no filter) for each filter versus the filter's %LT. Figure 6 shows the resulting plot corresponding to filter performance when using a CMOS camera to image a faint H-α rich nebula under a range of sky darkness levels, from a NELM of +2.9 (Bortle 9+) down to +6. Note that these are theoretical predictions of the increase in visible contrast between the object and the background. The absolute values of my predictions may not reflect what a user will experience with their own setup, but the predicted relative performance of one filter to another should be representative. In general, the desired performance for a filter is high contrast increase and high %LT, so the higher and more to the right a filter's performance is in the plot the better. Similar plots of predicted contrast increase for the other object types can be found in Appendix A.

For emission-type nebulae, the old rule of "narrower is better" is evident in the contrast increase plots. Filters are predicted to produce progressively better contrast the narrower the band pass, and thus the smaller the %LT. The Quad-ALP has a %LT slightly smaller than the UHC filter, and thus is predicted to produce slightly better contrast than that filter, but not as good as the GNB or NB-1 which have lower %LTs. On galaxies (see plots in Appendix A) the filters with pass bands in the near-IR are predicted to produce the best contrast increase. The Quad-ALP is predicted to perform slightly behind the AHC and GNB in this regard. On reflection nebulae the predicted increase in contrast is relatively small, on the order of +30 to +40%. All the filters tested are predicted to perform similarly on reflection nebulae, with the Quad-ALP showing the best performance when under severe light polluted skies. Filter performance on comets is predicted to be very similar to what was predicted for galaxies. By analysis the best contrast on comets comes from imaging them in the near-IR band. I have not had an opportunity to confirm this prediction with images of an actual comet.

Also calculated using my prediction method is the image SNR, as shown in Figure 7. Plots for all of the different object types are provided in Appendix B. The predicted SNR values are normalized so that the SNR with no filter equals 1.0, and it is assumed that the same sub-exposure time is used for each filter. Based on my predictions, the image SNR delivered by the different filters trends the same way as the contrast increase for emission-type nebulae – narrower bands and thus smaller %LT is better. For the other three object types however, broad spectrum emitters, better SNR is predicted the larger the %LT. In fact all the filters are predicted to have SNR values below 1 (worse than no filter) on broad spectrum targets when sub-exposure time is kept the same. A table summarizing all predicted filter performance values is provided in Appendix C, including the prediction of SNR when sub-exposure time is increased corresponding with filter %LT so that the same overall frame exposure is achieved.

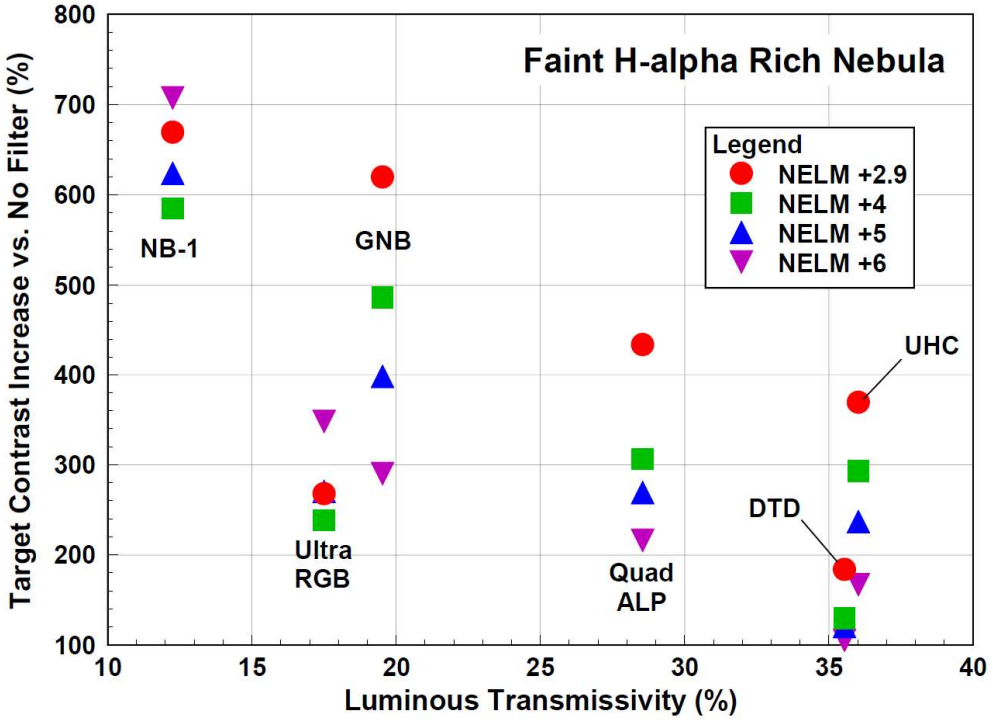

Figure 6 Predicted Filter Performance – Contrast Increase, Faint H-α Rich Nebula

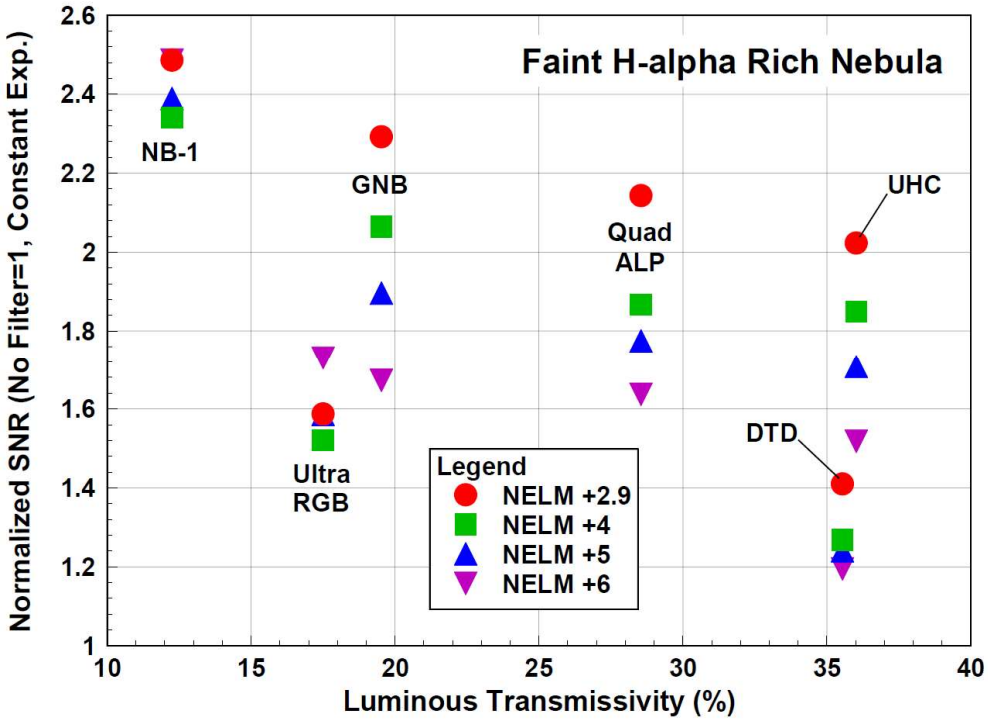

Figure 7 Predicted Filter Performance – SNR w/Fixed Exposure Time, Faint H-α Rich Nebula

Results - Imaging:
All image collection on a particular target was done within a 45-minute time window. This process was repeated multiple times, each on a different target as described above. Images were generated by live stacking in Sharpcap, with enough sub's captured in each case to generate a stack with 5 to 6 minutes (300-360s) total exposure. All the images had their histograms adjusted in exactly the same way using Fitswork v4.47, a free FITS editing software, so that they provide as fair a visual comparison as possible. Adjustments were made primarily for white balancing, but a small amount of non-linear stretch was also applied to enhance the visibility of the nebulosity or other faint details in the images. Images were also run through GraXpert to remove any gradients, and to do a final tweak to white balance. No image calibration was applied to the sub-exposures.

Images from the three imaging sessions are shown in Figures 8 to 15. The differences between filters are most evident when the target is an emission-type nebula (eg. Figures 9, 11, 14 &15). For this object type the increase in contrast that can be realized using a filter is large, so the impact on the image of using a filter is rather obvious. As expected, nebula contrast is best using the filter with the narrowest pass bands, the NB-1. On emission nebulae the Quad-ALP filter performed very similar to the GNB filter, which is more of an indication that the GNB did not perform as well as predicted than the Quad-ALP performing better than predicted.

When imaging galaxies (eg. Figures 8, 12 & 13) it was clear from the results that filters with a pass band in the near-IR do indeed produce a higher contrast. The Quad-ALP filter performed very similar to the UHC filter, which is better than predicted. On reflection nebulae (eg. Figures 10 & 15) the filters tested performed very much like what was predicted, with the Quad-ALP showing the largest increase in contrast. The improvement in contrast in reflection nebulae, although measurable, was relatively small as predicted.

Using the raw captured image data I was able to directly measure the contrast increase delivered by each filter, putting a number to what was already observed qualitatively from the images in Figures 8 and 15. This was accomplished by using AstroImageJ to measure the average luminance from common areas in the images: a dark background area, and a bright deepsky object target area. The particular areas used are illustrated in Figures 16 and 17 (red box for target, blue box for background), with these same areas used for all the images from the various filters. Measurements of luminance average and standard deviation were taken from the original unedited FITS files in each colour channel. Contrast increase was calculated from the measured luminance values using the following equations:

$$\text{Measured Contrast} = [\text{measured target luminance} - \text{measured background luminance}] \div \text{measured background luminance}$$

$$\%\ \text{Contrast Increase} = [\text{contrast w/filter} - \text{contrast w/out filter}] \div \text{contrast w/out filter} \times 100$$

Figure 8 Oct. 30th Imaging Results – M31 Andromeda Galaxy

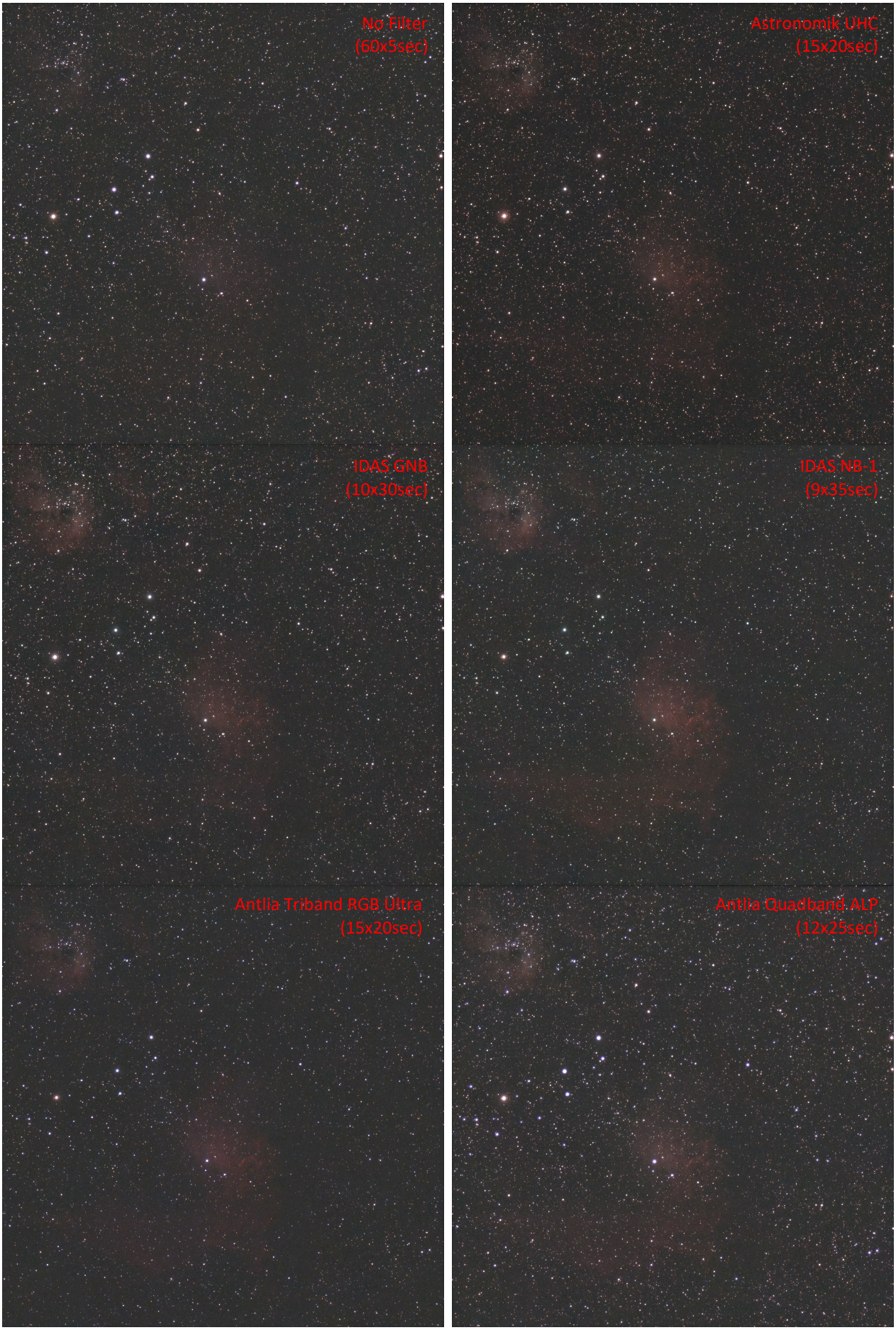

Figure 9 Nov. 10th Imaging Results – IC405 Flaming Star Nebula

Figure 10 Nov. 10th Imaging Results – M45 The Pleiades

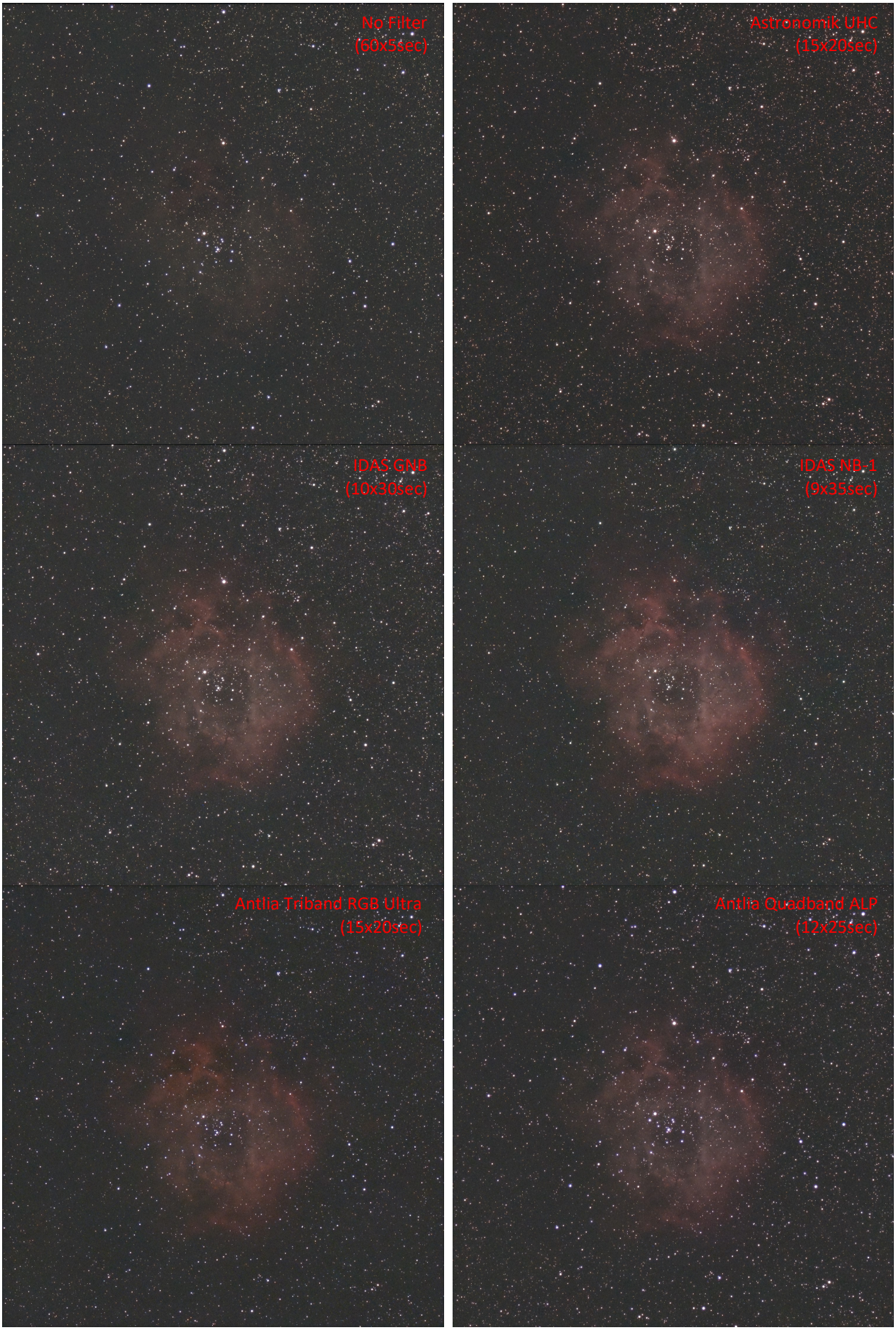

Figure 11 Nov. 10th Imaging Results – NGC2244 Rosette Nebula

Figure 12 Nov. 12th Imaging Results – M31 Andromeda Galaxy

Figure 13 Nov. 12th Imaging Results – M33 Triangulum Galaxy

Figure 14 Nov. 12th Imaging Results – NGC2024 Flame & B33 Horsehead Nebulae

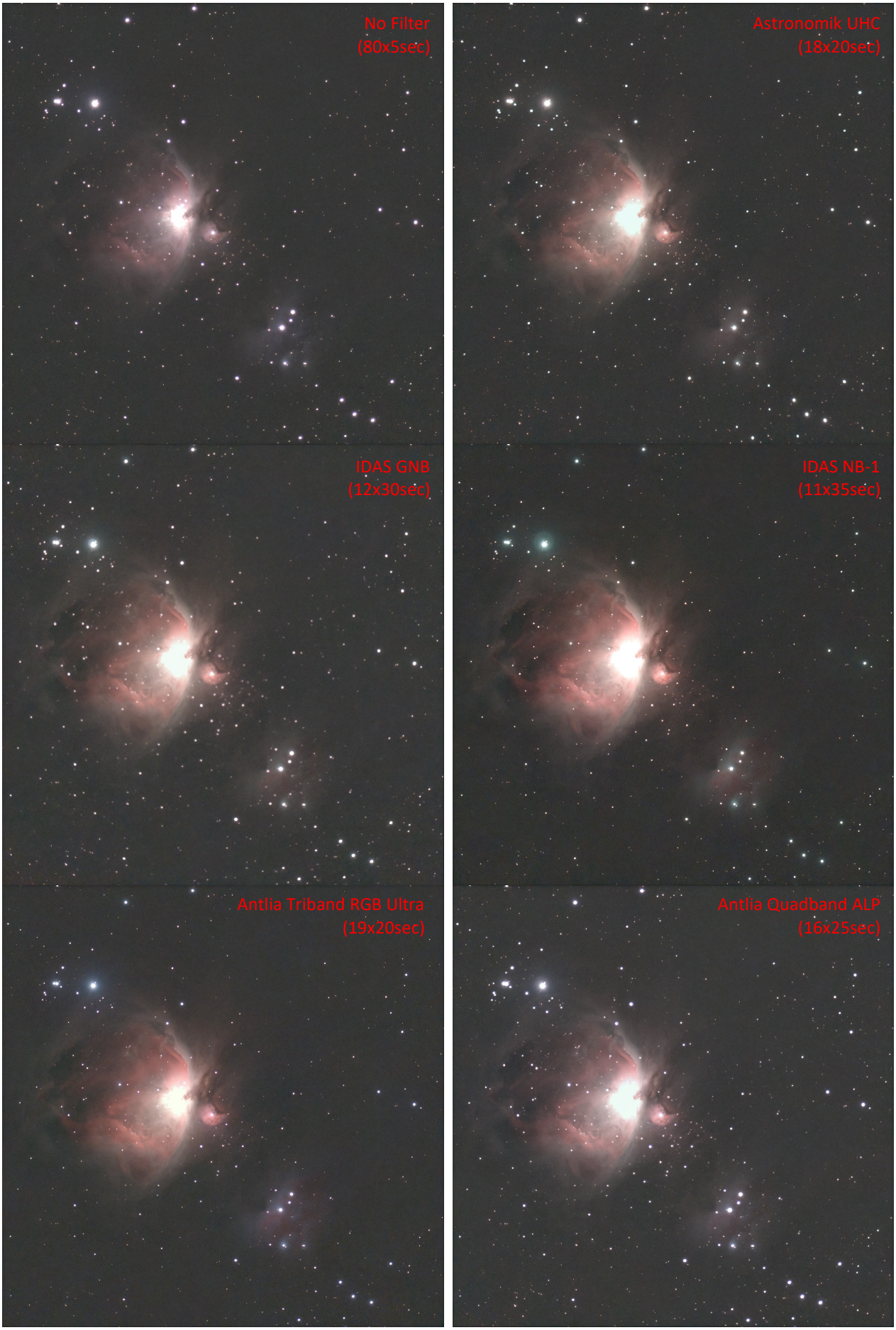

Figure 15 Nov. 12th Imaging Results – M42 Orion & NGC1977 Running Man Nebulae

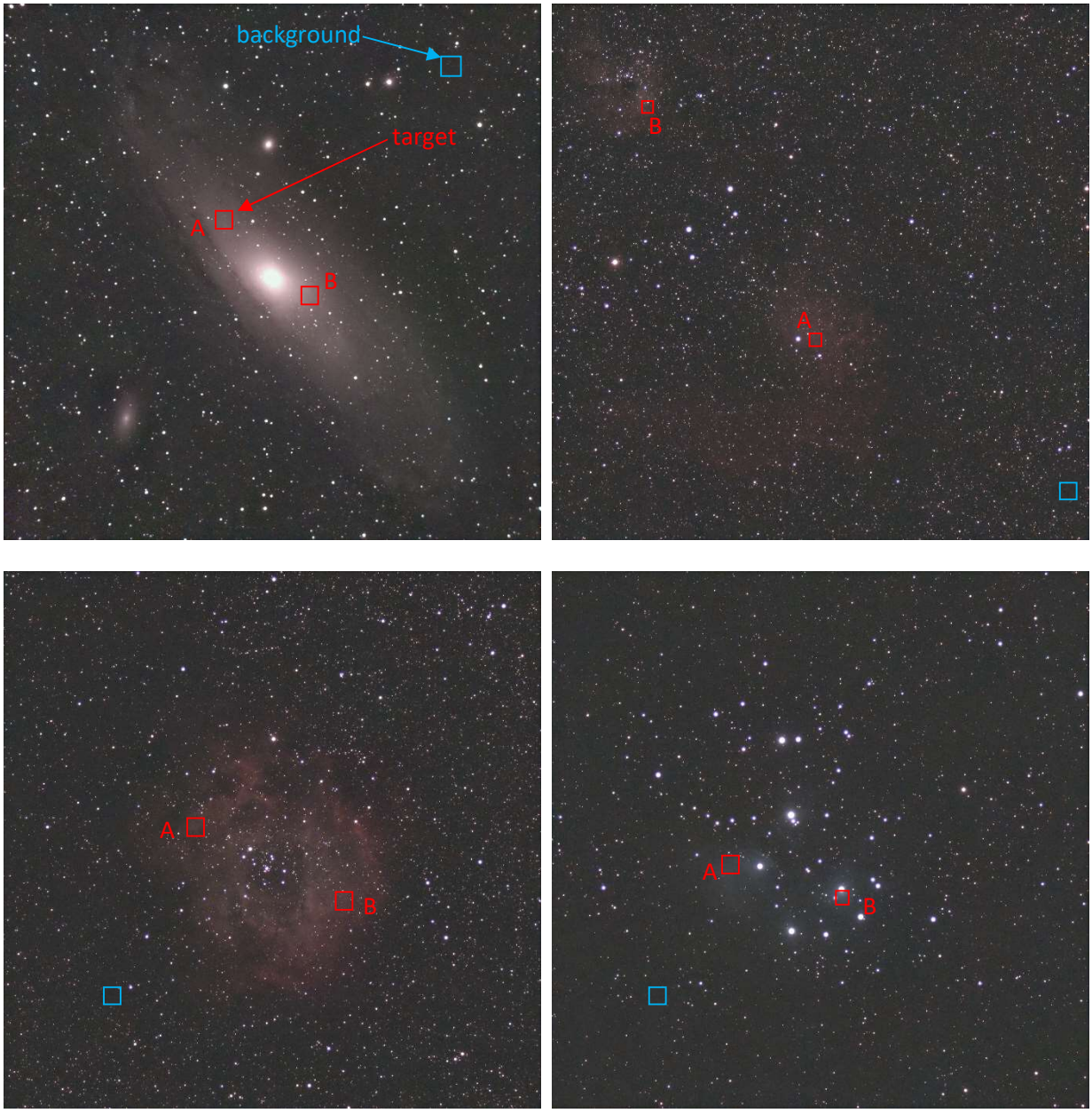

Figure 16 Areas Used for Image Analyses – Part 1

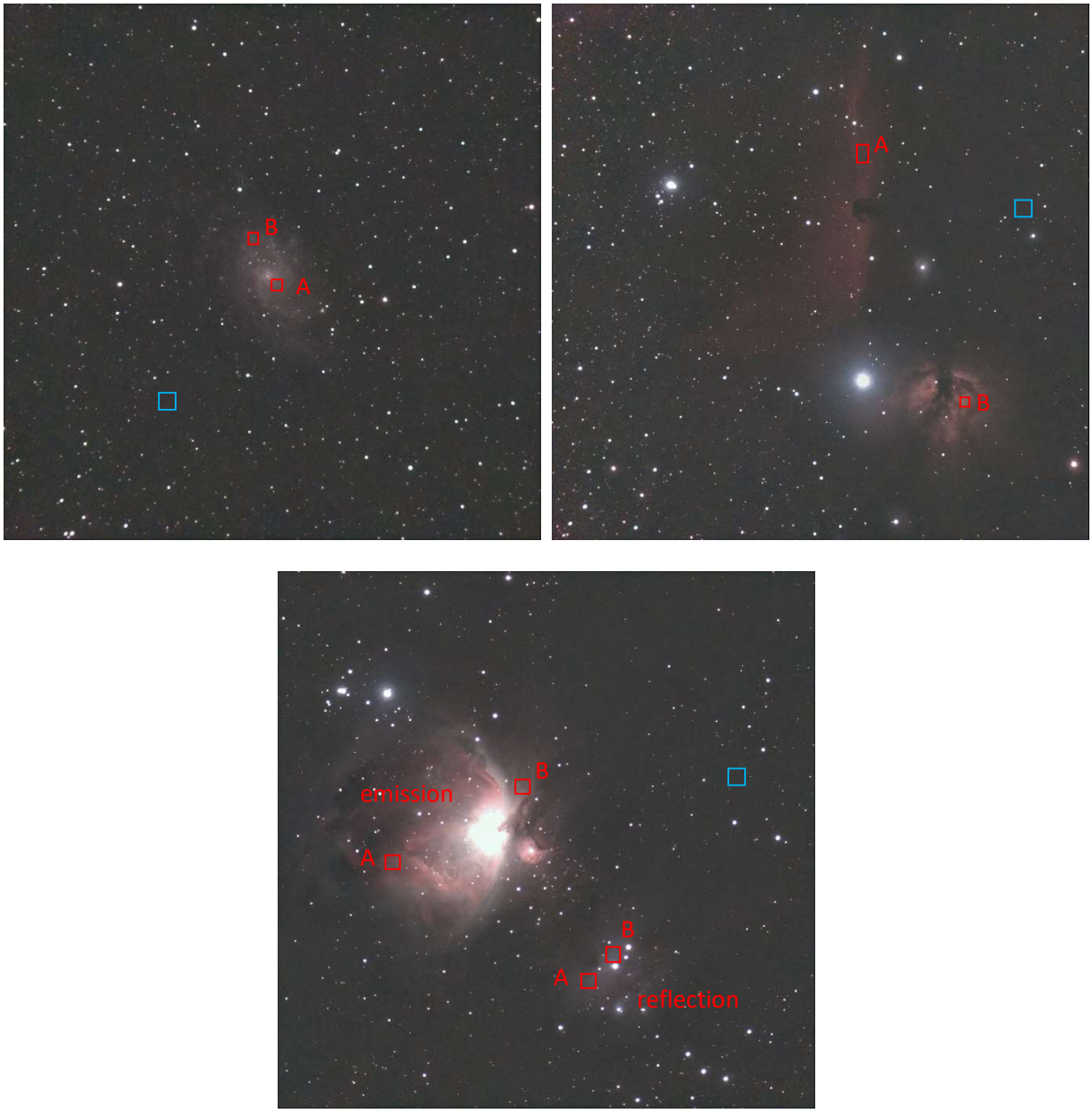

Figure 17 Areas Used for Image Analyses – Part 2

The resulting contrast increase measurements are plotted in Figures 18 to 20, along with the corresponding prediction for each filter. Some offset between measured contrast values and the predictions is expected since the sky conditions during the imaging session (i.e. transparency) is likely not going to be the same as what was assumed in the prediction calculations. It will also be the case that the object imaged will have a different magnitude (brightness) than the object used for the prediction. That being said, the relative performance of one filter compared with another is expected to be the same whether it was determined by analysis or measurement.

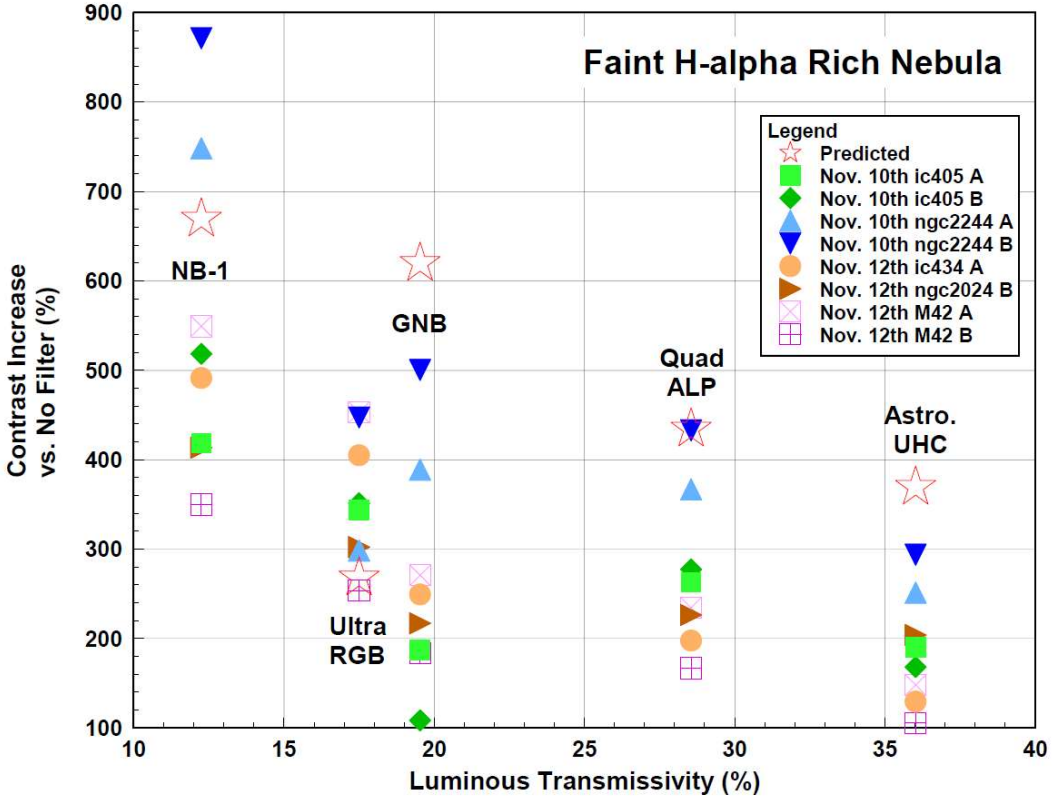

Figure 18 Measured Deepsky Object Contrast Increase vs. Predicted – Faint H-alpha Rich Nebula

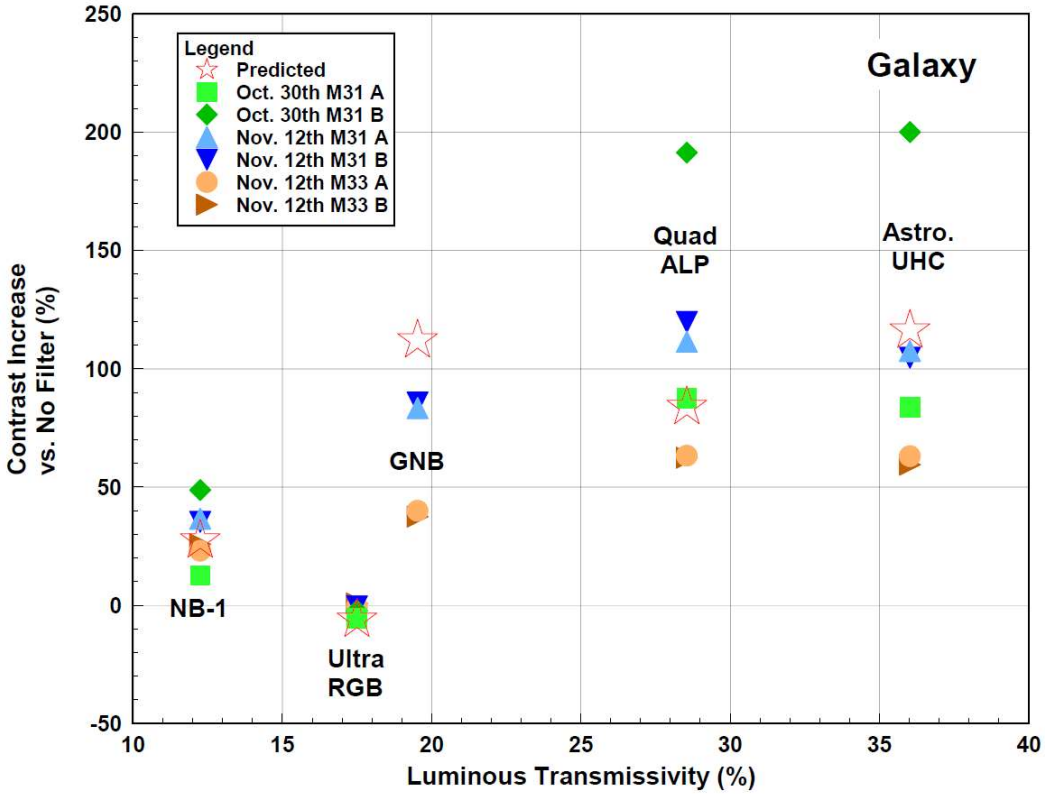

Figure 19 Measured Deepsky Object Contrast Increase vs. Predicted – Galaxy

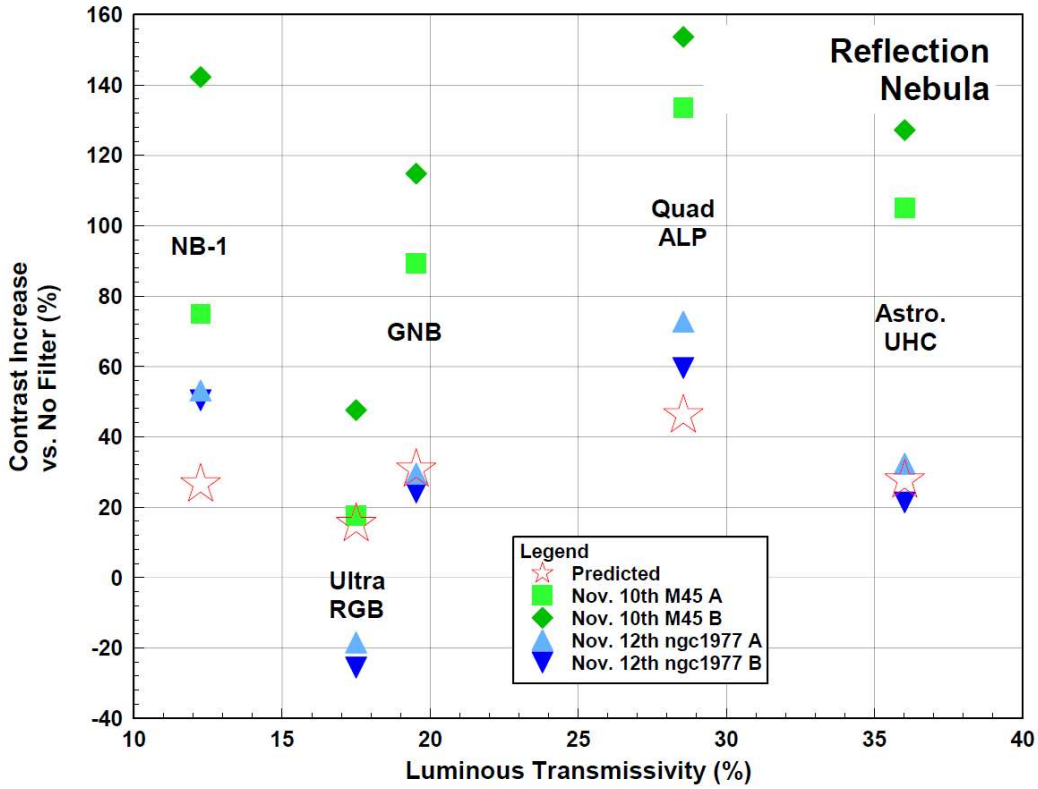

Figure 20 Measured Deepsky Object Contrast Increase vs. Predicted – Reflection Nebula

On faint H-α rich nebulae (Figure 18), most of the filters performed as predicted. The exceptions were the GNB which performed more poorly than predicted, and the RGB Ultra which performed better than predicted. The Quad-ALP was observed to perform better than the UHC on emission nebulae, and about the same as the GNB and RGB Ultra. The NB-1 was the best performing filter on emission nebulae, as expected based on the predictions.

On galaxies (Figure 19), the RGB Ultra and NB-1 performed almost exactly as predicted. The GNB performed worse than predicted, and the Quad-ALP performed better than predicted, in fact about the same as the UHC which was predicted to perform the best on galaxies.

On reflection nebulae (Figure 20), all five filters were predicted to perform about the same, with a slight advantage given to the Quad-ALP. This prediction was confirmed by the image data, although depending on the object the increase in contrast that was achieved was found to be much larger than predicted.

The measurements of luminance from the images also allowed me to evaluate signal-to-noise ratio (SNR). When I extracted the average luminance values from each image in AstroImageJ, I also recorded the standard deviation (σ). This allowed me to calculate the SNR achieved by each filter using the following equation:

SNR = (measured object luminance – measured background luminance) ÷ measured object σ

The normalized SNR measurements (no filter = 1.0) are presented in Figures 21 to 23.

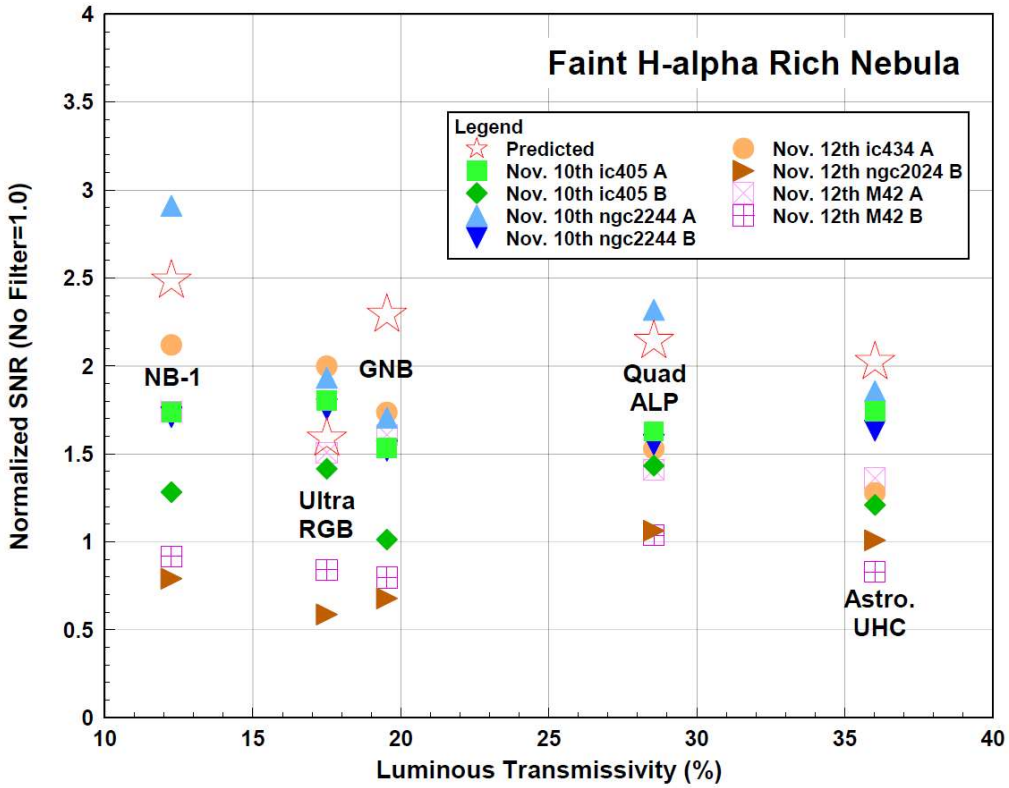

Figure 21 Measured Deepsky Object SNR vs. Predicted – Faint H-α Rich Nebula

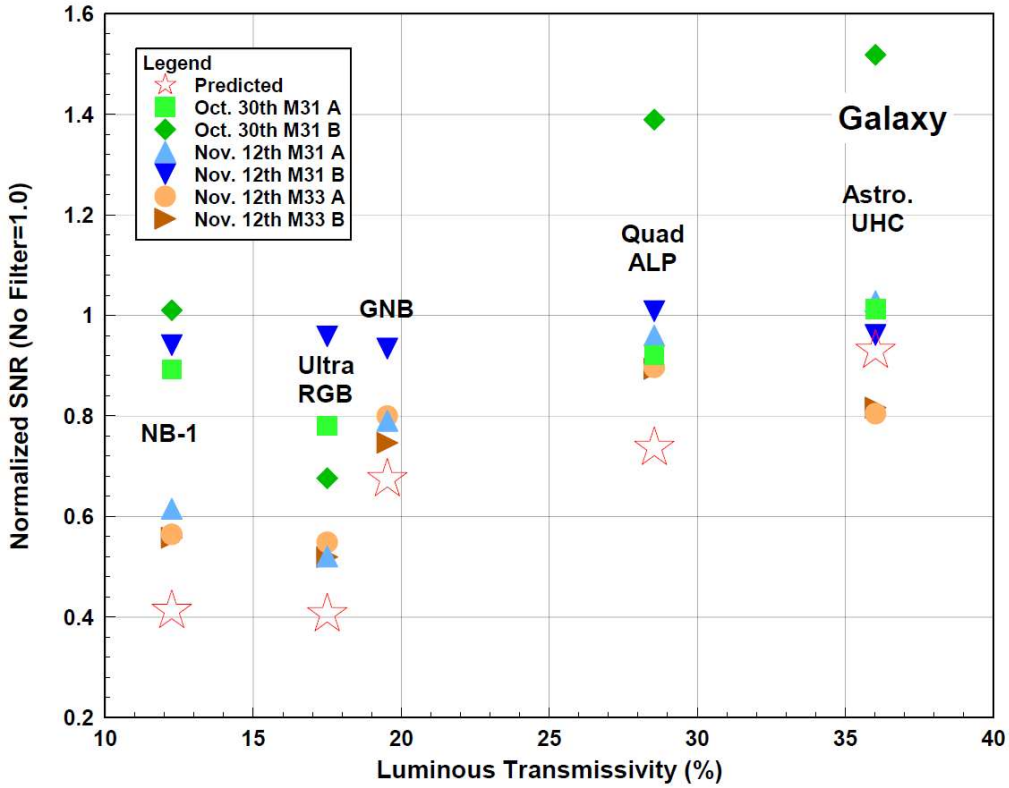

Figure 22 Measured Deepsky Object Contrast Increase vs. Predicted – Galaxy

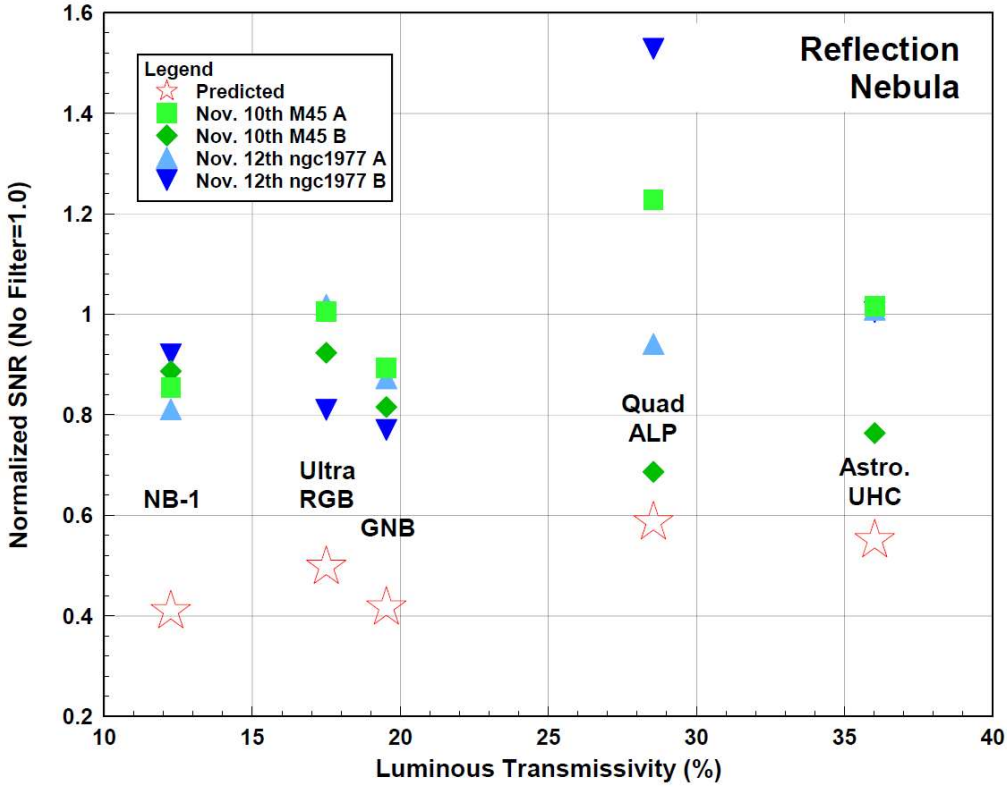

Figure 23 Measured Deepsky Object Contrast Increase vs. Predicted – Reflection Nebula

As with the contrast increase measurements, the measured SNR shows a significant amount of scatter due to the variation in observing conditions and target brightness. For all the different object types however, the trend in the predicted SNR aligns well with the measured data. On H-α rich nebulae (Figure 21) the GNB and NB-1 filters performed below what was predicted, resulting in the SNR produced by the Quad-ALP being comparable to those two filters which were predicted to be superior. On galaxies (Figure 22) all the filters produced an SNR level that was consistent with the prediction except the Quad-ALP, which performed slightly better than predicted. A similar observation was made for reflection nebulae (Figure 23), the Quad-ALP performing slightly better than predicted while all the other filters performed as expected.

One of the other things noted during the image collection process, and subsequent processing afterwards, was how well white balanced the images produced using each filter are. To provide an impression of how well white balanced each filter's image was at the time of data collection, consider the versions of my November 12th M31 captures in Figure 24. These are the raw stacked images with no post-processing applied, and with their corresponding histogram added to the lower right corner. The camera colour channel gains were not touched between filters from those used for the no filter case which has a relatively well colour balanced histogram.

As one might expect, having an image's colour channel histograms spread out like shown for some filters in Figure 24 has an impact on processing the image data after-the-fact. When the colour channel histogram peaks are closer together, the image is much easier to white balance than when they are far apart.

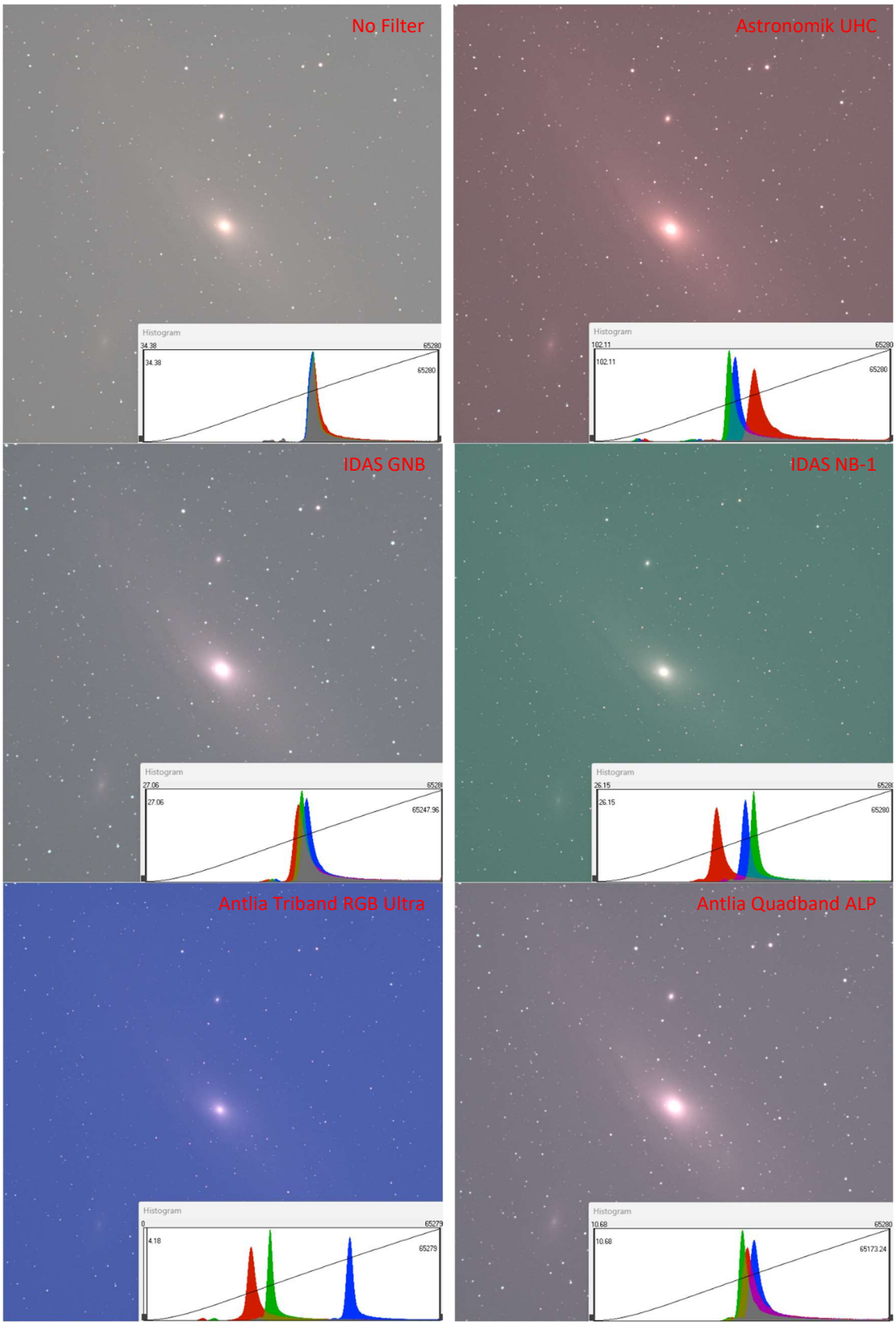

Figure 24 Comparison of Raw Stack Colour Balance

Another aspect of using the filter affected by their white balance is how that impacts the selection of sub-exposure time. I have found that filters that produce a large disparity in the location of each colour channel's histogram peak are difficult to set a proper exposure time for. For example, when the blue channel histogram is located far to the right from the red channel histogram, it is challenging to get enough exposure on the red channel without saturating the blue channel. The RGB Ultra was the worst of the filters tested in this regard.

Several other observations were made from the image data that was collected, as summarised below:

- Halos were observed around bright stars for most of the filters tested. The Quad-ALP did exhibit some halos, but they were pretty faint compared to the other filters that had halos (see Figures 25 and 26).
- Hot blue stars have a slightly swollen appearance when using the Quad-ALP filter compared to the others tested. This was most apparent when I was imaging M45 (see Figure 10 above). This is probably due to a combination of the fact that the Quad-ALP filter passes some near-UV, an emission that is prevalent in hot blue stars, and it may be the case that the refractor I used was not able to perfectly focus the near-UV light at the same time as the light from the other filter pass bands.
- When imaging with the ZS66 scope I found that stars looked a little out of focus for all of the filters with a pass band in the near-IR, including the Quad-ALP. The ZS66 is an ED-doublet refractor, so it is very likely not capable of focusing visible and NIR light at the same time. Images captured using the FMA230, a triplet refractor, did not show any issues with achieving a good focus.
- The plastic case used by Antlia for all of their filters is not practical. It is needlessly larger than most other filter cases, and it does not close securely. After receiving the Antlia filter from the vendor, I immediately moved it to a better case.

Figure 25 Examples of Halos Around Bright Stars – Alcyone (+2.85, 12,258K)

Figure 26 Examples of Halos Around Bright Stars – σ Orionis (+4.00, 35,000K)

Conclusions:
Based on the results of the testing described above, I have made the following conclusions:

1. Based on my predictions of filter performance, which are based on the filter transmission spectra that I measured using a spectrometer, the IDAS GNB filter is the best all-round general purpose filter (refer to summary table in Appendix C). The new Antlia Quadband ALP filter is predicted to perform the best on reflection nebulae, but is predicted to perform below the GNB on all other object types. The imaging results however indicated that the Quad-ALP performs better than my predictions, and the GNB worse than my predictions. Therefore, the Quad-ALP in fact appears to be the best all-round filter.
2. The Quad-ALP filter produces some haloing around bright stars, but I would not consider the halos strong. Halos produced by the GNB and NB-1 filters were significantly worse. The Quad-ALP filter also produced slightly bloated hot blue stars due to it passing some near-UV light.
3. Filters like the Quad-ALP, which have pass bands in the near-IR range along with the visual range of wavelengths, are more challenging for optics to focus properly. The ED-doublet refractor I used for imaging tests was not able to focus the Quad-ALP properly, but the triplet APO refractor I used was. Although not tested, I would expect that reflecting-type telescopes would not have an issue focusing with the Quad-ALP filter.
4. There was a discrepancy observed between my contrast predictions and what was measured from my test images, the magnitude of which was larger than what I typically see during these sorts of tests. I am wondering now if maybe the way I perform my prediction calculation has something to do with the discrepancy. The calculation is presently performed assuming a monochrome sensor. It may be the case that to achieve more accurate predictions of contrast increase when using a OSC camera will require me to perform the calculation three times, once for each colour channel.

If you have any questions, please feel free to contact me.

Cheers!

Jim Thompson
(top-jimmy@rogers.com)

Appendix A – Predicted Increase in Object Contrast vs. No Filter

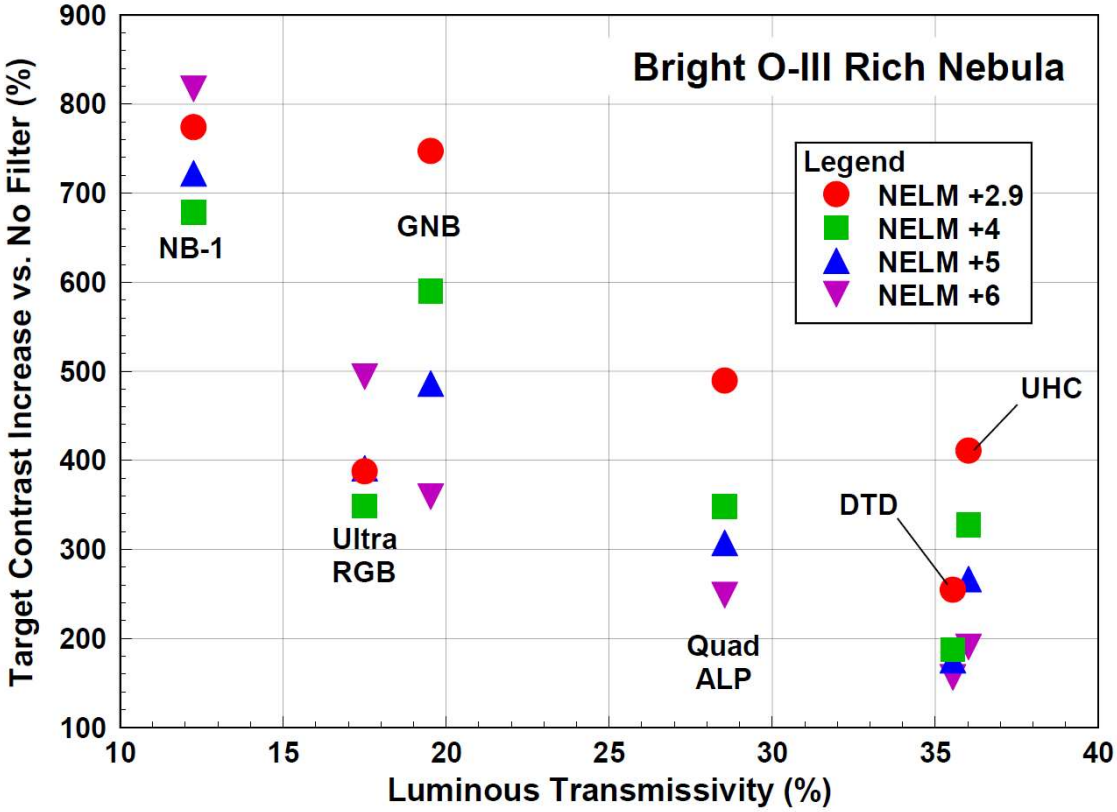

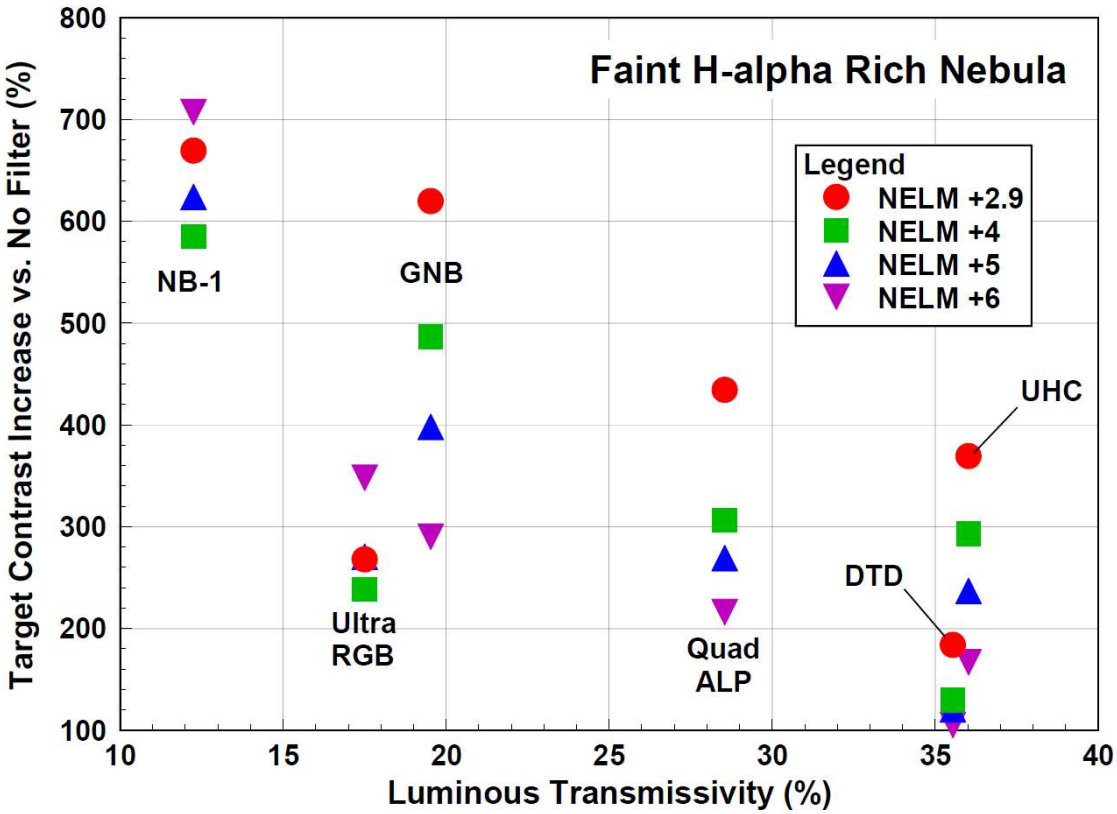

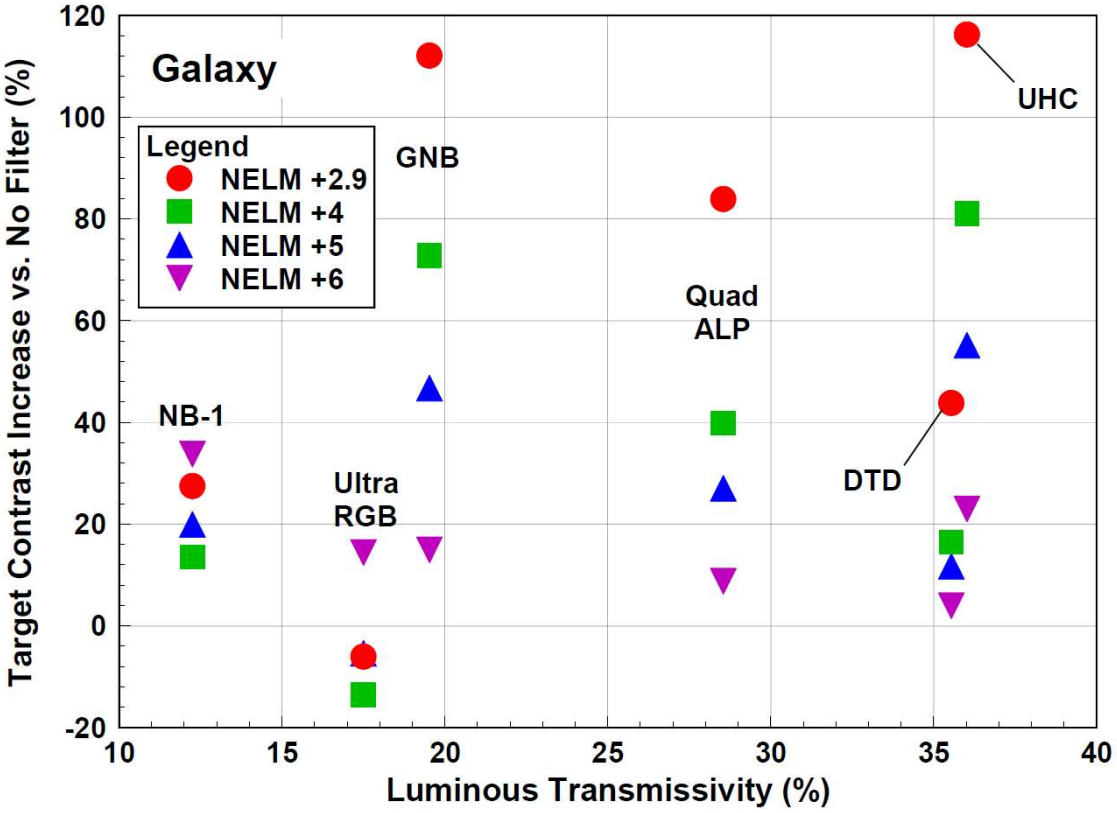
Galaxy
Legend
NELM +2.9
NELM +4
NELM +5
NELM +6
GNB
UHC
Quad
ALP
NB-1
Ultra
RGB
DTD
Target Contrast Increase vs. No Filter (%)
Luminous Transmissivity (%)
120
100
80
60
40
20
0
-20
10
15
20
25
30
35
40

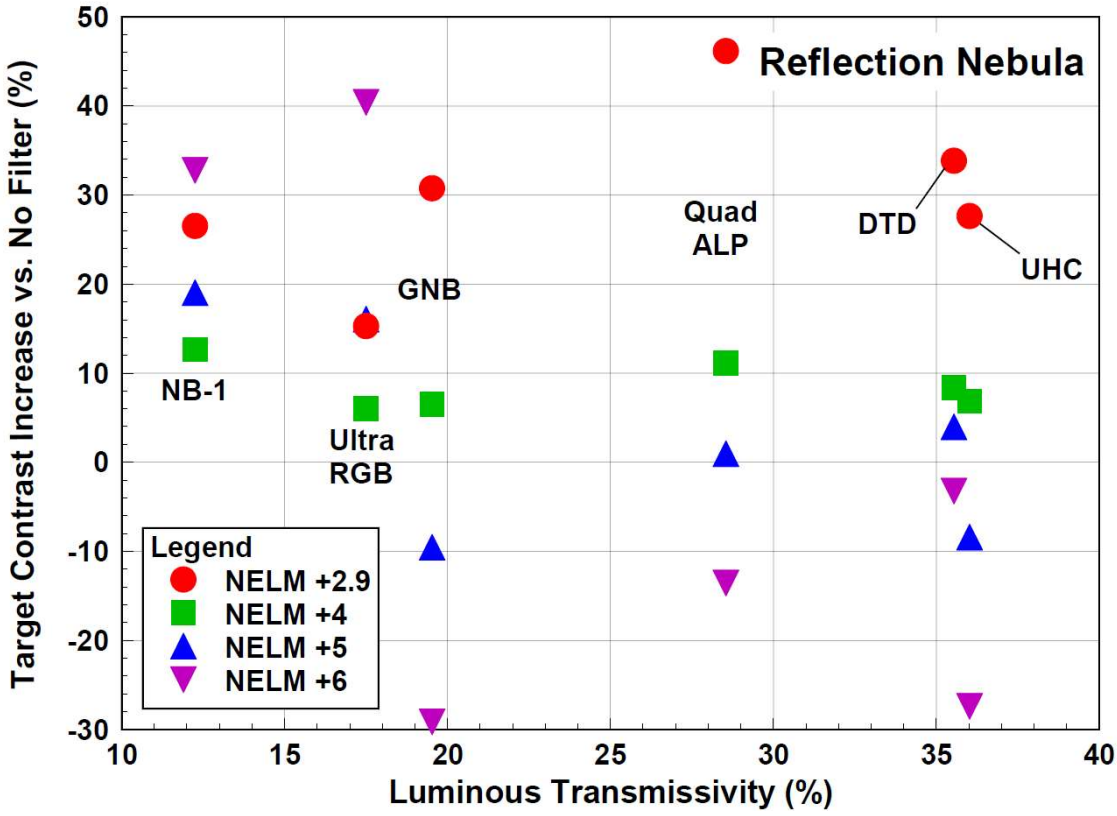
Reflection Nebula
Quad
ALP
DTD
UHC
GNB
NB-1
Ultra
RGB
Legend
NELM +2.9
NELM +4
NELM +5
NELM +6
Target Contrast Increase vs. No Filter (%)
Luminous Transmissivity (%)
50
40
30
20
10
0
-10
-20
-30
10
15
20
25
30
35
40

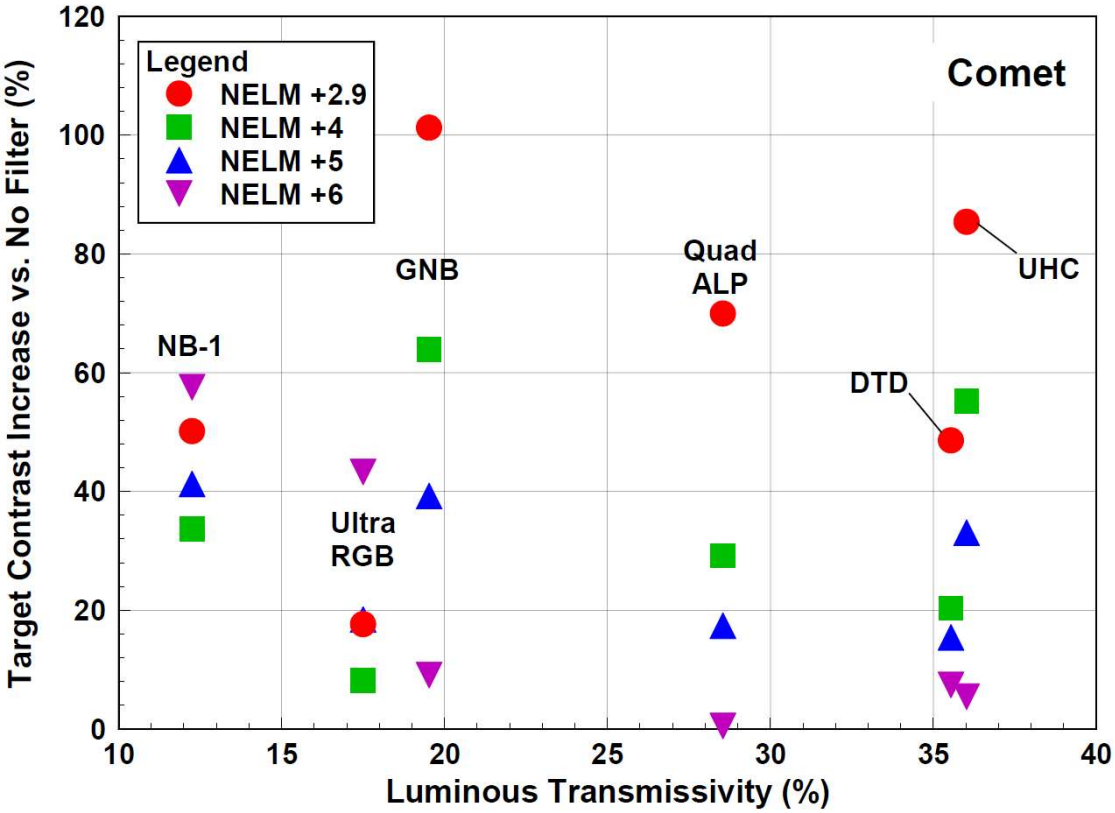
Comet
Legend
NELM +2.9
NELM +4
NELM +5
NELM +6
Target Contrast Increase vs. No Filter (%)
Luminous Transmissivity (%)
120
100
80
60
40
20
0
10
15
20
25
30
35
40
NB-1
GNB
Ultra
RGB
Quad
ALP
DTD
UHC

Appendix B – Predicted Normalized SNR for Constant Sub-Exposure Time

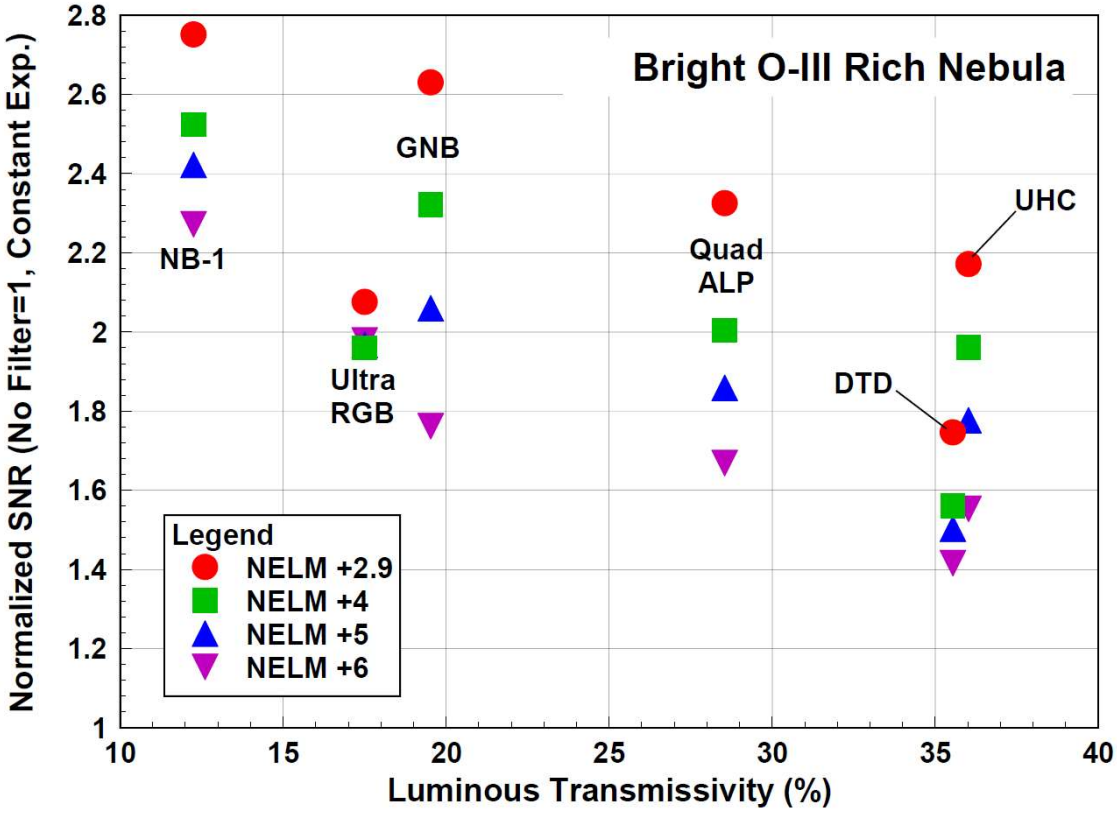

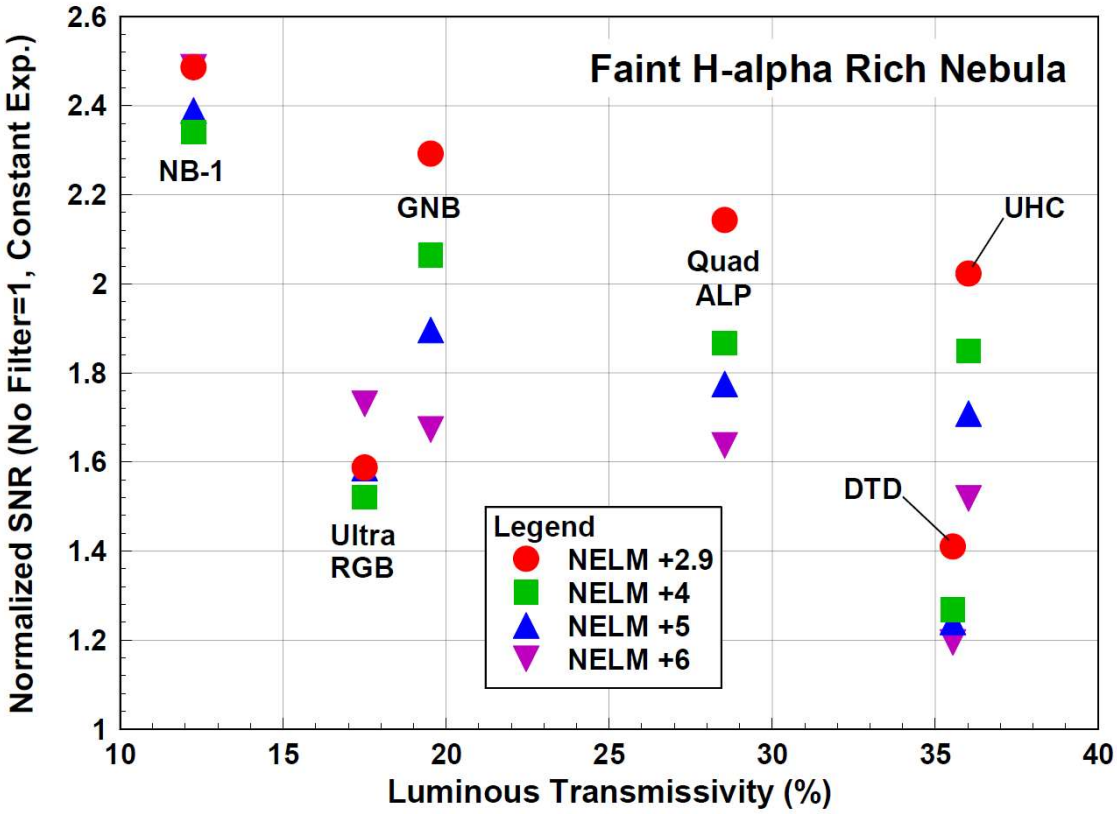

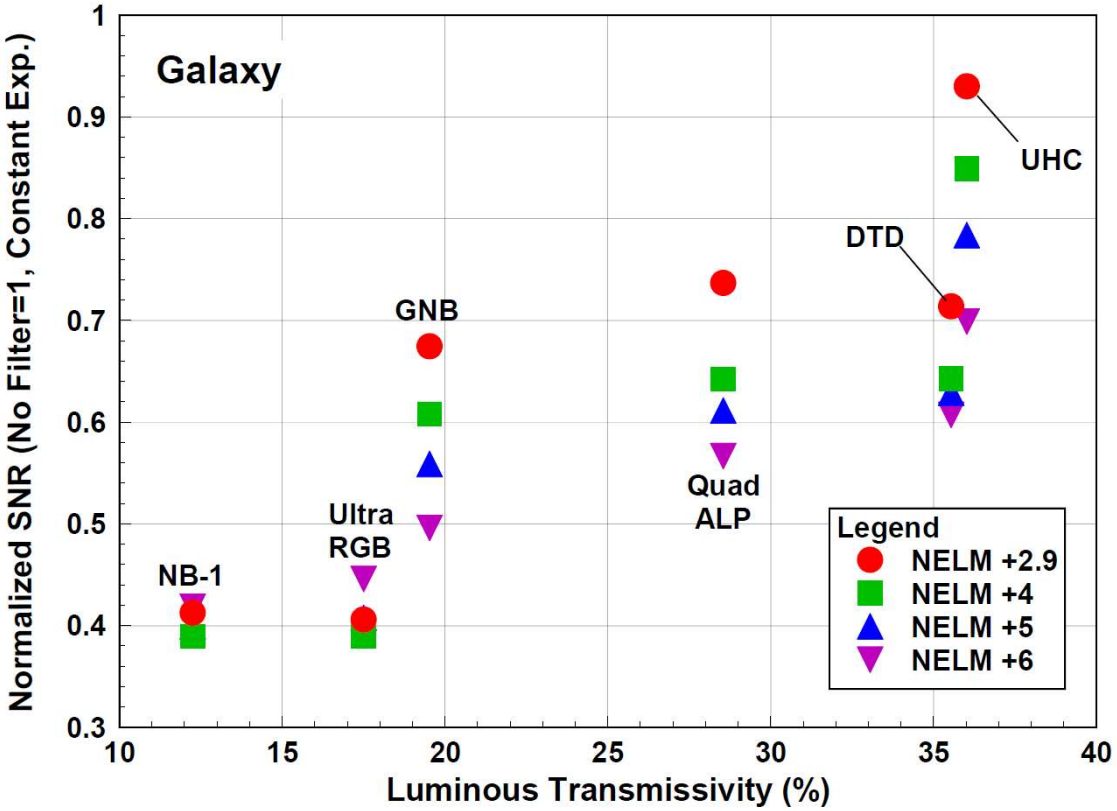
Galaxy
Normalized SNR (No Filter=1, Constant Exp.)
Luminous Transmissivity (%)
NB-1
Ultra RGB
GNB
Quad ALP
DTD
UHC
Legend
NELM +2.9
NELM +4
NELM +5
NELM +6

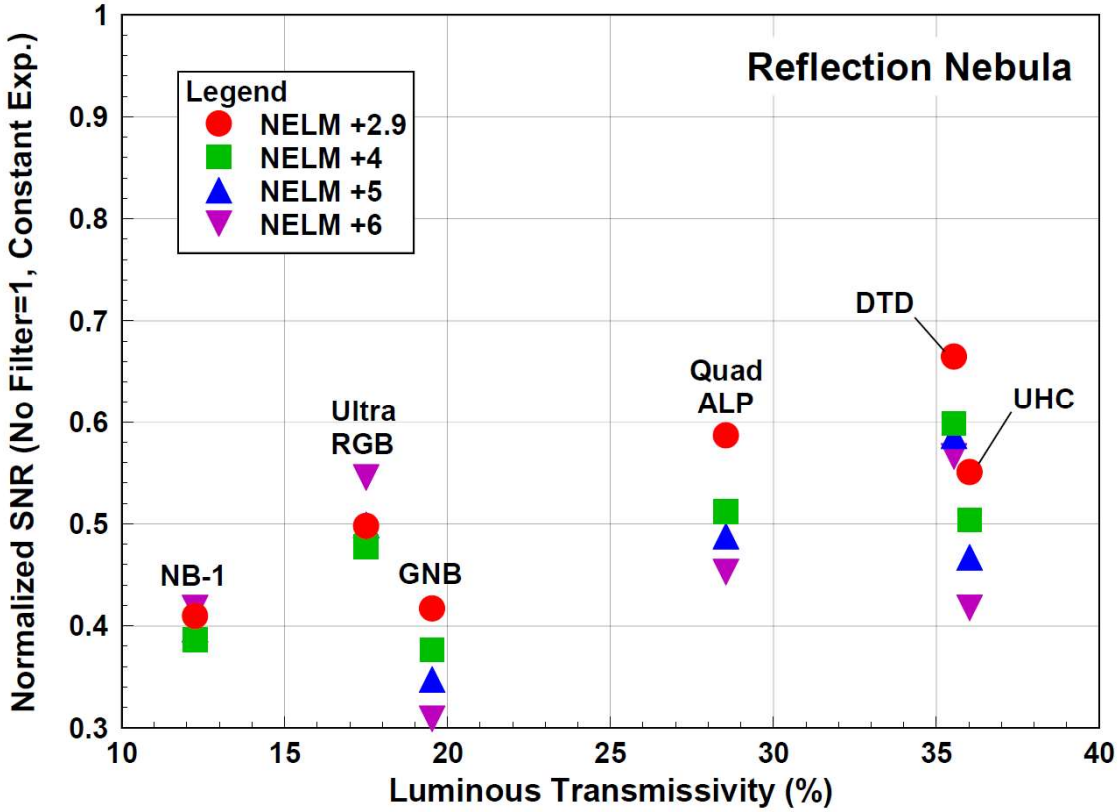
Reflection Nebula
Normalized SNR (No Filter=1, Constant Exp.)
Luminous Transmissivity (%)
Legend
NELM +2.9
NELM +4
NELM +5
NELM +6
NB-1
Ultra RGB
GNB
Quad ALP
DTD
UHC

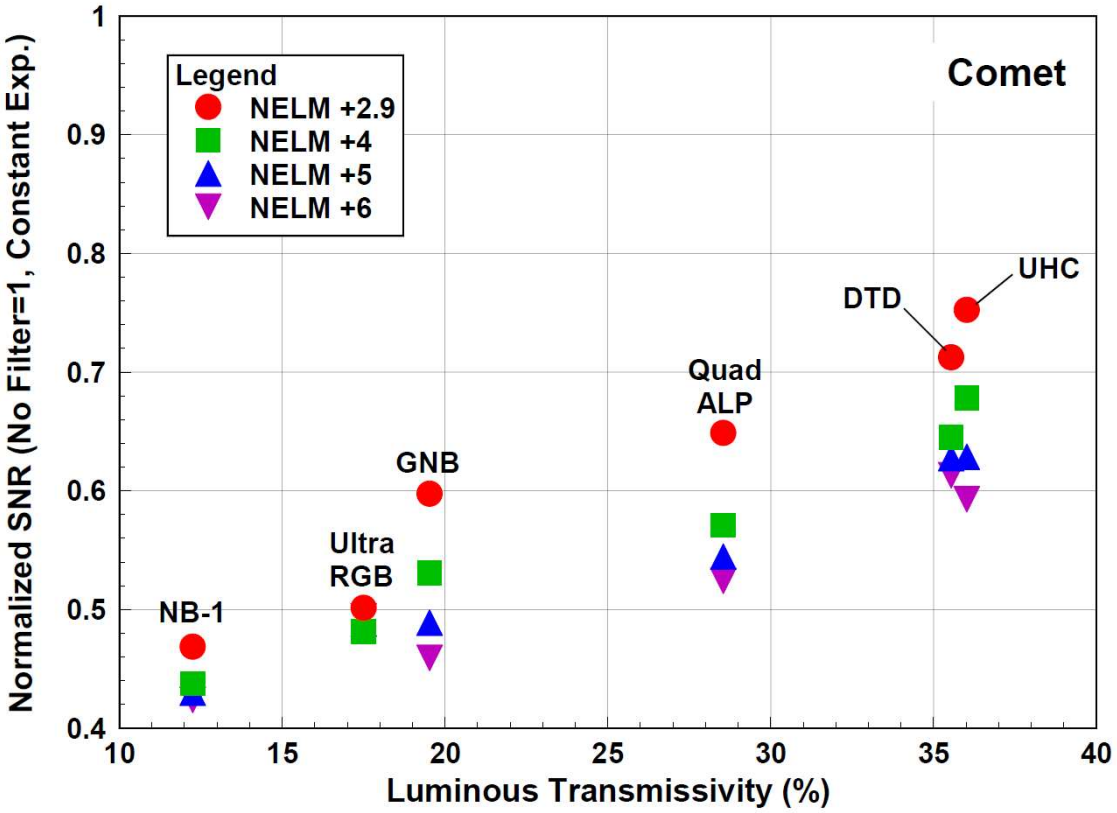
Comet
Legend
NELM +2.9
NELM +4
NELM +5
NELM +6
NB-1
Ultra RGB
GNB
Quad ALP
DTD
UHC
Normalized SNR (No Filter=1, Constant Exp.)
Luminous Transmissivity (%)
1
0.9
0.8
0.7
0.6
0.5
0.4
10
15
20
25
30
35
40

Appendix C – Summary Table of Predicted Filter Performance

Performance Parameter	Object	NELM	No Filter	Astro-nomik UHC	IDAS DTD	IDAS GNB	IDAS NB-1	Antlia Ultra RGB	Antlia Quad ALP
Luminous Transmissivity (%)			100.00	36.02	35.54	19.53	12.25	17.50	28.55
% Contrast Increase vs. No Filter	Bright O-III Nebula	MAG+2.9		410.86	254.64	747.27	774.00	387.60	489.50
		MAG+4		327.71	187.18	590.22	678.31	348.53	348.24
		MAG+5		266.62	175.49	486.11	722.24	390.95	307.19
		MAG+6		190.55	156.37	359.19	817.12	493.88	248.67
	Faint Halpha Nebula	MAG+2.9		369.32	183.83	619.88	669.41	267.88	434.35
		MAG+4		292.93	129.84	486.44	585.17	238.40	306.30
		MAG+5		236.80	120.49	397.99	623.85	270.40	269.10
		MAG+6		166.92	105.19	290.15	707.38	348.06	216.05
	Galaxy	MAG+2.9		116.24	43.80	112.10	27.47	-6.06	83.90
		MAG+4		81.05	16.45	72.78	13.52	-13.58	39.83
		MAG+5		55.18	11.71	46.72	19.92	-5.41	27.03
		MAG+6		22.99	3.96	14.95	33.76	14.42	8.77
	Reflection Nebula	MAG+2.9		27.64	33.84	30.75	26.53	15.28	46.15
		MAG+4		6.87	8.38	6.51	12.67	6.04	11.13
		MAG+5		-8.40	3.97	-9.55	19.03	16.07	0.96
		MAG+6		-27.40	-3.24	-29.14	32.77	40.41	-13.55
	Comet	MAG+2.9		85.40	48.58	101.25	50.14	17.63	69.95
		MAG+4		55.23	20.32	63.95	33.70	8.21	29.22
		MAG+5		33.05	15.42	39.22	41.25	18.44	17.39
		MAG+6		5.45	7.41	9.07	57.54	43.27	0.52
Fixed Sub-Exposure Time SNR	Bright O-III Nebula	MAG+2.9	1.00	2.17	1.75	2.63	2.75	2.08	2.33
		MAG+4	1.00	1.96	1.56	2.32	2.52	1.96	2.00
		MAG+5	1.00	1.78	1.50	2.06	2.42	1.97	1.86
		MAG+6	1.00	1.55	1.42	1.76	2.27	1.98	1.67
	Faint Halpha Nebula	MAG+2.9	1.00	2.02	1.41	2.29	2.49	1.59	2.14
		MAG+4	1.00	1.85	1.27	2.07	2.34	1.52	1.87
		MAG+5	1.00	1.71	1.24	1.90	2.39	1.59	1.77
		MAG+6	1.00	1.52	1.19	1.67	2.49	1.73	1.64
	Galaxy	MAG+2.9	1.00	0.93	0.71	0.67	0.41	0.41	0.74
		MAG+4	1.00	0.85	0.64	0.61	0.39	0.39	0.64
		MAG+5	1.00	0.78	0.63	0.56	0.40	0.41	0.61
		MAG+6	1.00	0.70	0.61	0.50	0.42	0.45	0.57
	Reflection Nebula	MAG+2.9	1.00	0.55	0.66	0.42	0.41	0.50	0.59
		MAG+4	1.00	0.50	0.60	0.38	0.39	0.48	0.51
		MAG+5	1.00	0.47	0.59	0.35	0.40	0.50	0.49
		MAG+6	1.00	0.42	0.57	0.31	0.42	0.55	0.45
	Comet	MAG+2.9	1.00	0.75	0.71	0.60	0.47	0.50	0.65
		MAG+4	1.00	0.68	0.65	0.53	0.44	0.48	0.57
		MAG+5	1.00	0.63	0.63	0.49	0.43	0.49	0.54
		MAG+6	1.00	0.59	0.61	0.46	0.42	0.49	0.52

Optimized Sub-Exposure Time SNR	Bright O-III Nebula	MAG+2.9	1.00	5.03	3.51	8.24	8.49	4.81	5.79
		MAG+4	1.00	4.16	2.83	6.57	7.35	4.35	4.35
		MAG+5	1.00	3.49	2.66	5.37	7.25	4.57	3.85
		MAG+6	1.00	2.71	2.42	4.06	7.19	5.06	3.19
	Faint Halpha Nebula	MAG+2.9	1.00	4.69	2.84	7.18	7.68	3.68	5.34
		MAG+4	1.00	3.92	2.30	5.84	6.82	3.38	4.05
		MAG+5	1.00	3.35	2.20	4.94	7.15	3.69	3.67
		MAG+6	1.00	2.65	2.04	3.86	7.86	4.42	3.13
	Galaxy	MAG+2.9	1.00	2.15	1.44	2.11	1.27	0.94	1.83
		MAG+4	1.00	1.80	1.16	1.72	1.13	0.87	1.39
		MAG+5	1.00	1.54	1.11	1.46	1.20	0.95	1.26
		MAG+6	1.00	1.22	1.04	1.14	1.32	1.14	1.08
	Reflection Nebula	MAG+2.9	1.00	1.28	1.34	1.31	1.26	1.15	1.46
		MAG+4	1.00	1.07	1.08	1.06	1.13	1.06	1.11
		MAG+5	1.00	0.92	1.04	0.91	1.19	1.16	1.01
		MAG+6	1.00	0.73	0.97	0.71	1.32	1.39	0.87
	Comet	MAG+2.9	1.00	1.74	1.43	1.87	1.45	1.16	1.62
		MAG+4	1.00	1.44	1.17	1.50	1.27	1.07	1.24
		MAG+5	1.00	1.23	1.11	1.27	1.29	1.13	1.13
		MAG+6	1.00	1.04	1.05	1.06	1.34	1.26	1.00